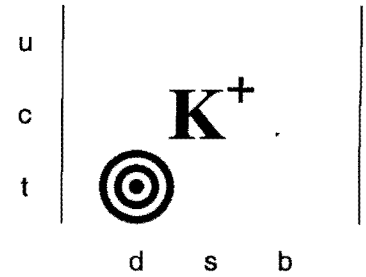

K*plus* - A Cost Effective and Competitive Precision Measurement of the Decay $K^+ \to \pi^+\nu\overline{\nu}$

April 7, 2005

CKM Collaboration *

Abstract

At last April's Fermilab PAC meeting the CKM collaboration presented a redesign and adaptation of the CKM technique from the proposed new separated kaon beam facility to an unseparated beam experiment, renamed **K***plus* , that can be mounted in the existing KTeV facility. The overall sensitivity goal of the primary measurement remains 100 $K^+ \to \pi^+\nu\overline{\nu}$ signal events with a small background. This sensitivity is achieved by exploiting both low-background kinematic regions available in the $K^+ \to \pi^+\nu\overline{\nu}$ decay. The **K***plus* physics program consists of the primary measurement of the $K^+ \to \pi^+\nu\overline{\nu}$ decay amplitude to a precision limited by theoretical uncertainties and a suite of rare and precision studies in both K^+ and π^+ decays. The π^+ decay physics is a new opportunity made possible by the large π^+ flux in the unseparated beam.

The technical questions raised last April have now been addressed. The **K***plus* measurement is feasible for the 25-30M$ TPC cost range indicated then. In the past year KTeV's sister experiment at CERN, NA48, has come to the same conclusion. That collaboration with the NA48/3 experiment is now proceeding toward the same physics goals with a very similar technique. The CERN management is largely supportive and foresees no substantial obstacles for providing beam to the NA48/3 experiment in 2009-2010 assuming it continues to advance along a successful path.

The CKM collaboration has now reached a critical cross-roads. We propose here to either advance a competitive program for this physics here at Fermilab or to abandon kaon physics at Fermilab and join with our CERN colleagues to advance this physics in Europe. The requirements for the former path are a time competitive R&D program to re-establish a kaon facility at Fermilab with existing facilities and equipment in order to demonstrate the critical performance parameters in the charged kaon beam and measure the actual background sources there. This R&D program would proceed in parallel with the national reviews necessary for the approval of the project required to construct the new apparatus necessary to execute the measurement. This is exactly NA48/3's plan: they are scheduled for such beam next year while they complete their full proposal.

* Spokesman: Peter S. Cooper, Fermilab MS234, *pcooper@fnal.gov*

1 Introduction

Our major physics goal is a low background measurement of the branching ratio of the ultra-rare charge kaon decay $K^+ \to \pi^+\nu\overline{\nu}$ with statistical precision approaching 10%. Within the Standard Model this measurement provides the theoretically cleanest determination of the parameter $|V_{td}|$. It is one of the most sensitive tests of the Standard Model description of quark flavor mixing. Any significant deviation from the Standard Model predictions based upon existing and expected measurements in the b-quark sector is clear, model independent, evidence for physics beyond the Standard Model. This remains one of the most important unachieved measurements in high-energy physics.

In an era of potential new signals from the LHC input from the suite of precision measurements in quark flavor physics will be crucial in interpreting any new discoveries. For example, the maze of super-symmetric models and parameters will not be fully illuminated by only a short list of initial signals and modes from the LHC experiments. Precision deviations, or non-deviations from the Standard Model predictions will put important limits on all models.

If supersymmetry or other new physics is discovered at the LHC understanding the flavor structure of this new physics is of great importance. The question as to whether the flavor structure of this new physics is governed by the Standard Model Yukawa couplings (Minimal Flavor Violation, MFV) or whether there are new sources of CP violation and a new flavor structure, requires data from experiments such as **K***plus* . If no new physics is discovered at the LHC precise measurements of clean quantities in flavor physics will remain a critical probe of physics beyond the Standard Model.

Grossman has observed that the cleanliness of $K^+ \to \pi^+\nu\overline{\nu}$ and $K_L^0 \to \pi^0\nu\overline{\nu}$ comes from the neutrinos in the final state and the strength of isospin symmetry. These modes are not only clean in the Standard Model, but also in any MFV model and in many other models. Fits to CKM parameters will not establish new physics unless those fits fail. Isidori's has noted that all Standard Model CKM data is from tree-level or $\Delta Flavor = 2$ processes. New precise data on $\Delta Flavor = 1$, like are available from $K^+ \to \pi^+\nu\overline{\nu}$ and $K_L^0 \to \pi^0\nu\overline{\nu}$, may contain the clues to new physics that we are now missing.

Our approach, originally CKM(E921), has been rigorously reviewed and approved by numerous expert technical panels, the Fermilab PAC, and Directorate. In the end, the national P5 review, which could not identify sufficient funds for us to mount CKM(E921), characterizes it as an "*elegant world-class quark flavor physics experiment*".

We are unwilling to abandon a world class piece of physics which we are well positioned to undertake and achieve. The confluence of this financial impasse and recent demonstrations in very high rate tracking detector technology have presented us with the opportunity to adapt our original technique to a more cost effective solution. We can exploit, to much greater degree, existing facilities and equipment; thus substantially reducing the additional resources required to successfully make this measurement.

This adaptation is a trade-off of higher beam flux for a much less challenging photon system. Neither approach is risk-free. The new design offers a larger range of affordable mitigations making it, if not a better, at least a more adaptable, technique. This comparison is discussed in detail in Section 11 below.

The nature and status of our original design was summarized for the DOE Facilities Panel Review in February 2003 [1]. This document will well serve the reader as a succinct primer and reminder of the original CKM(E921) plans. Complete details are available in our proposal [2] and on our web-site [3]. Our submission and presentation to the April 2004 Fermilab PAC can be found on the web at [4,5]. At the time of that status report we outlined a redesign of the experiment and

enumerated a set of critical questions which had to be answered in order to evaluate the feasibility of the technique. This document is a revision of that work which includes affirmative answers in place of those questions.

We summarize here a redesign of CKM for a $K^+ \to \pi^+\nu\overline{\nu}$ experiment in an unseparated beam utilizing the existing KTeV beam line and experimental hall at Fermilab. For definiteness we will call this design **K***plus* . The original, approved, Fermilab E921 experiment with a separated $22GeV/c$ kaon beam in the MP beam line and MP9 detector hall will be called CKM here.

In short, it is feasible with this approach to achieve the same physics goal as in CKM: a measurement of the branching ratio of $K^+ \to \pi^+\nu\overline{\nu}$ with a statistical uncertainty and background fraction both approaching 10%. There are significant advantages in the **K***plus* design relative to CKM: in particular the photon veto requirement are much easier to achieve and therefore substantially cheaper. We present a detailed comparison of the two techniques below. Tracking ~ 20 pions and protons nearly in-time with each beam kaon is a formidable challenge. We present below a demonstration based on detector performance observed in the beam at CERN under similar conditions which demonstrates this challenge to be tractable.

Our primary physics goal is a determination of the $K^+ \to \pi^+\nu\overline{\nu}$ decay amplitude to a precision limited by the uncertainty in the mass of the charmed quark. The large pion flux in the unseparated beam adds to the additional measurements in K^+ decay, which we have enumerated in the CKM(E921) proposal, an expanded range of additional rare and precision measurements in π^+ decay.

The recent establishment of direct CP violation in the neutral kaon system ($Re(\epsilon'/\epsilon)$) was based on high energy kaon beam experiments which are now excellent candidates for evolution to the **K***plus* design. The SCRF beam separation system central to the CKM design required a relatively low energy beam and detector design. Relaxing this constraint, at the cost of handling a beam with 4% kaons rather than 60%, makes the **K***plus* design feasible in the KTeV experiment as well as the NA48 beam and apparatus at CERN. Adaptations similar in character to those developed here for the KTeV beam line and detector would also be required for NA48 beam and apparatus. This effort is now underway as NA48/3.

1.1 The National Review of CKM(E921) by P5

CKM(E921) was reviewed by the P5 panel in the spring and summer of 2003 in the context of only two new projects, both at Fermilab; BTeV and CKM. Each had been approved and advanced by Fermilab. The full text of P5's recommendations are reproduced below.

> "Evaluation - The subpanel was impressed with the excellent work of the proponents on the design of the experiment and their successful prototyping results. CKM is an elegant world-class experiment, which would be able to produce important physics results. However, the committee assigns it a lower priority than the BTeV experiment. The main reason is that BTeV has a much broader physics program at a comparable cost."
>
> "Suggestions Based on Prioritization - The present Fermilab plan calls for a similar funding profile and time-line for BTeV and CKM construction with both starting to take data around 2009. The P5 Subpanel believes that this plan is likely to be too ambitious given the need to optimize the physics from the Tevatron Collider, as well as the desire to have BTeV completed promptly. 'Based on current budgetary models, P5 does not recommend proceeding with CKM.'"

After recent cancellation of the BTeV project the K*plus* proposal we are making here; at 1/3 the original CKM cost and 1/6 the cost of BTeV, has to be re-evaluated in the light of these recommendations,the present realities in both fiscal and human terms at Fermilab, and with the presence of real competition from CERN for this science now.

1.2 Collaboration

The CKM collaboration remains largely intact. The only group to leave us after our rejection by P5 in September 2003 was the University of Colorado group. They felt compelled to take this action after discussions with the DOE regarding their future funding in the wake of the P5 decision.

All the other groups remain. Most of them have actively contributed to this work. Doubling the size of the collaboration is necessary to execute this experiment successfully. However, with the indeterminate state of CKM for the past 18 months we have been unwilling to actively recruit new collaborating institutions.

We have spoken with many of our colleagues outside of CKM. We are confident that adding several more University groups is achievable when we can go to them with demonstrated, positive, actions by both Fermilab and the DOE so that there is good reason to believe that K*plus* will move forward as an experiment and that grants will not be at risk from participation in the collaboration. They same argument is valid for expanding the collaboration membership within the four collaborating laboratories.

1.3 Competition

We are now in a competition with the NA48/3 effort at CERN for a measurement of the $K^+ \rightarrow \pi^+\nu\overline{\nu}$ branching ratio. This collaboration has successfully completed two years of data taking with a charged kaon beam on NA48/2 - the search for CP violation in the comparison of the $K^\pm \rightarrow \pi^+\pi^-\pi^\pm$ Dalitz plots. They have just announced a preliminary result from their 2003 data [6]. The KABES ultra high rate beam tracker was developed for this experiment and was used during this run. It was not yet incorporated into the analysis for their preliminary result.

This collaboration has submitted a letter of intent at the CERN Villars workshop last September to undertake a competitive measurement of the $K^+ \rightarrow \pi^+\nu\overline{\nu}$ branching ratio using their existing beamline with a modified apparatus [7, 8]. Their design is still evolving but is essentially similar to ours. As presently conceived, they require a $860MHz$ narrow-band unseparated beam flux at $70GeV/c$ which has a 6% kaon content.

Their upstream tracking and kaon tagging is a combination of KABES, very high rate Silicon pixels and a tagging Cherenkov counter. Downstream redundant decay pion tracking is done with drift chambers in a two magnet double-bend spectrometer. Photon vetoes use their existing liquid Krypton photon calorimeter in addition to new vacuum photon veto modules. A new muon veto system is under consideration; muon background from $K^+ \rightarrow \mu^+\nu_\mu$ is an important problem in the present design.

NA48/3's general plan is to turn the detector back on in 2006 in order to test and validate components of the new experiment. They will evolve toward complete detector ready for physics data beginning around 2009-10. Discussions we have had with the CERN management indicate that CERN is prepared to support and provide beam at that time to such an effort provided it makes good progress toward full approval and has suitable external support for the detector upgrades. CERN sees no important problems in providing either the beam or funds for an appropriate CERN fraction of the detector. The CERN viewpoint is that the physics case is compelling. They perceive the the present size of the collaboration to be a weakness of the proposal. In our discussions with

both the NA48/3 collaboration and the CERN management we have been actively encouraged and invited to join this effort. If necessary most of us are prepared to do so.

2 Physics Motivation and Reach

2.1 Physics Goals

2.1.1 $K^+ \to \pi^+\nu\overline{\nu}$

We require an experiment designed to measure the branching ratio of $K^+ \to \pi^+\nu\overline{\nu}$ with physics sensitivity comparable to the original CKM experiment with a separated beam: ~ 100 signal events for a branching ratio of 1×10^{-10} with $<\sim 10\%$ background acquired with $2-3$ years of data taking. The motivation for a $\sim 5-6\%$ statistical uncertainty in the $K^+ \to \pi^+\nu\overline{\nu}$ decay amplitude is to match the theoretical uncertainty, estimated at $\sim 5\%$, in this amplitude due to uncertainty in the mass of the charmed quark. Work now in progress on NNLO corrections should be able to improve this theoretical uncertainty to the $\sim 3\%$ level [9].

New work since the CKM proposal to expand the phase space of the search for $K^+ \to \pi^+\nu\overline{\nu}$ allows us to include both low-background regions; PNN1 as before and a PNN2 region between $K^+ \to \pi^+\pi^0$ and the onset of three body decays. This provides an additional observable not contained in the original CKM proposal. The ratio of the number of signal events observed in these two regions is a measure of the form-factor in the $K^+ \to \pi^+\nu\overline{\nu}$ decay mode. The form-factor is predicted to be identical to that in $K^+ \to \pi^0 e^+\nu_e$ decays. The precision achievable in this ratio would only be 25% in **K***plus* , but if the $K^+ \to \pi^+\nu\overline{\nu}$ branching ratio were twice the Standard Model predicted value (as presently observed in BNL E787/949, albeit with a large statistical uncertainty) this ratio could be quite valuable in sorting out possible beyond-the-Standard-Model hypotheses. Now that we understand that backgrounds can be controlled in "Region II", as we called PNN2 in the proposal, this ratio is equally measurable with the CKM technique, where we would have had twice the statistics of **K***plus* .

2.1.2 Pion Decay Physics

Rare pion decays have played an important role in limiting anomalous scalar, pseudo-scalar, and tensor couplings through precision measurement of the helicity-suppressed $\pi^+ \to e^+\nu_e$ and $\pi^+ \to e^+\nu_e\gamma$ decays. The helicity suppression constrains the Standard Model branching fraction of $\pi^+ \to e^+\nu_e$ to 1.2×10^{-4}, providing a window for amplitudes from virtual high mass exchanges arising from physics beyond the Standard Model to compete in the total branching fraction.

$$R_{\pi_{l2}} = \frac{\Gamma[\pi^+ \to e^+\nu_e\ (\gamma)]}{\Gamma[\pi^+ \to \mu^+\nu_\mu\ (\gamma)]} \tag{1}$$

The expected ratio of $R_{\pi_{l2}}$ (equation 1) can be calculated reliably to the extraordinary precision of 0.05% [10]. This robust Standard Model prediction enables precision measurement of R_π to probe contributions from sources such as lepto-quarks at $200GeV$, lepto-quark compositness at $1TeV$, multiple Higgs models and TeV-scale Brane models. The ratio R_π is currently measured with a precision of 0.4%. This invites an experimental campaign to push this window by another factor of $\times 8$ to match the theoretical uncertainty.

New physics can be further probed by precision measurement of the $\pi^+ \to e^+\nu_e\gamma$ form factor. For center of mass photon energies greater than $10MeV$ the expected branching fraction is 5.5×10^{-7} [11]. The (V-A) based form factors of this decay are calculated to high precision which

provides extraordinary sensitivity to new amplitudes. New physics preferentially distorts the high photon energy region of the Dalitz plot, where the dominant inner bremsstrauhlung component is relatively small. The PiBeta experiment at PSI has recently reported precision measurements of a suite of rare pion decays [11, 12] including $\pi^+ \to e^+\nu_e\gamma$. PiBeta reports an intriguing departure from the expected (V-A) form factor of high statistical significance in the region of high photon energy [12]. This has motivated the PiBeta collaboration to propose further running to study this anomaly, which has recently been approved by PSI. Hints of this anomaly has been seen in previous experiments [13].

The latest round of precision rare pion decay measurements have been performed using stopped pions [14, 15]. The stopped-pion measurement uncertainties are now dominated by background and detector acceptance modeling estimations [11, 12, 14, 15]. The experiments have made careful estimates of these systematics errors based on a demonstrated understanding of detector performance. Nevertheless, further progress requires a technique with reduced or at least different systematic uncertainties which motivates consideration of an in-flight decay experiment. The large fraction of pions in the high intensity **K***plus* unseparated beam presents an opportunity to probe in-flight pion decays with unprecedented sensitivity. Stopped pion techniques by necessity are complicated by the presence of stopping material and measurement of low energy photons and electrons. In contrast, pion decays in the **K***plus* apparatus occur in vacuum and produce high energy ($\sim 10GeV$) decay electrons and photons that can be measured with very high precision with modern fully active calorimeters. The high flux of **K***plus* pions permits matching the statistical precision of previous pion decay measurements with three months of modest intensity Main Injector beam. The detector systems required for these measurements are a subset of the full complement of $K^+ \to \pi^+\nu\overline{\nu}$ instrumentation motivating consideration of a program of world-class pion decay measurements prior to full $K^+ \to \pi^+\nu\overline{\nu}$ running with the **K***plus* apparatus.

2.1.3 Other Kaon Decay Physics

In the CKM proposal [2, 16, 17] we demonstrated that the large kaon flux and excellent properties of the CKM spectrometer gave access to many rare kaon decays, with sensitivities approaching 10^{-12} in parallel with the main $K^+ \to \pi^+\nu\overline{\nu}$ program. The CKM apparatus included two high precision velocity (RICH) and magnetic spectrometers for both the incident kaon and charged decay products, a forward photon calorimeter and a muon detector, hermetic photon and muon veto coverage to suppress background processes, and a powerful trigger and DAQ system. The capability for precise measurement and identification of decay particles together with the suppression of background processes are quite important to kaon decay studies.

The general thrust of additional measurements are motivated by the search for new physical processes beyond the Standard Model. These include:

- Lepton flavor violation in kaon decays.
- New scalar, pseudo-scalar or tensor weak interactions in decays like: $K^+ \to e^+\nu_e$, $K^+ \to \pi^0 l\nu_l$, and $K^+ \to \pi^+ l^+ l^-$
- T-odd correlations in $K^+ \to \pi^0 l^+\nu_l\gamma$ decays.
- New low-mass particles in kaon decay like $K^+ \to \pi^+ S^0$, and $K^+ \to \pi^+\pi^0 P^0$ (sGoldstino)

There are also precision studies of low energy hadron physics in weak decays like:

- Radiative decays.

- $\pi\pi$ interactions in $K^+ \to \pi\pi l^+\nu_l$ decays.
- $\pi\pi$ interactions in $K^+ \to \pi^+\pi^0\pi^0$ decays.
- Form-factor studies.

These hadronic studies are important for further developments of lattice QCD, chiral perturbation theory, other hadronic models and quark confinement in general.

All of these studies remain feasible in the **K***plus* design with an unseparated beam. The details of these measurement are changed with the new geometric and kinematic conditions. These are being re-evaluated with the **K***plus* design. A disadvantage of **K***plus* is the reduction of 60% in the number of kaon decays studied with respect to CKM. This will reduce the statistical sensitivities of all measurements by this factor. At the same time however the kinematics in **K***plus* will greatly improve the measurement of π^0's in kaon decays with the CsI calorimeter. The **K***plus* kinematics and calorimeter performance can in many cases compensate the reduced kaon flux; for example, in decays like $K^+ \to \pi^0 l^+\nu_l\gamma$. For processes like $K^+ \to \pi^-\mu^+\mu^+$ where sensitivity is dependent on background suppression rather than total decay flux, the **K***plus* environment will not degrade the sensitivity expected in CKM.

As discussed previously, the **K***plus* experiment has sensitivity for new interactions that may be present in $\pi^+ \to e^+\nu_e$ and $\pi^+ \to e^+\nu_e\gamma$ decays. The analogous measurements in the kaon system are also sensitive probes of physics beyond the Standard Model. The **K***plus* experiment affords simultaneous measurements for both $R_{\pi_{l2}}$ and $R_{K_{l2}}$ (equation 2).

$$R_{K_{l2}} = \frac{\Gamma[K^+ \to e^+\nu_e\ (\gamma)]}{\Gamma[K^+ \to \mu^+\nu_\mu\ (\gamma)]} \tag{2}$$

These complementary studies can exploit the excellent environment of the **K***plus* apparatus to reduce the associated systematic uncertainties. These measurements have significant sensitivity for new types of interactions. For example, as was shown in [18,19], the measurement of $R_{K_{l2}}$ provides a precision test of $\mu - e$ universality, which can probe lepto-quark models up to $\Lambda_{LQ} > 150TeV$.

3 Costs

A requirement, in order to make this measurement feasible in the US, is to achieve this measurement at a substantially lower cost than the 101M$ cost assigned to CKM.

A re-estimation of the cost for CKM with maximum utilization of existing beam lines and enclosures at Fermilab and including the results of our test beam studies of photon veto and other prototypes has been made. Notable among the detector cost reductions is the vacuum veto subsystem, where the now-measured high energy inefficiency [20] allows the CKM veto requirements to be met with 1/2 the veto detector volume, corresponding to about a 50% reduction in sub-system cost. The re-estimated total CKM cost is in the $50 - 55M\$$ range in this model.

The largest cost subsystem remaining in the CKM design, after the changes above, is the separated kaon beam. These costs includes the SCRF separator cavities, RF power supply, superfluid liquid Helium cryogenics plant, civil construction required for the beam-line and cryo-plant, etc. These costs total $15 - 20M\$$ of the revised CKM cost estimate above.

An unseparated beam experiment in an existing area and beam-line can, by further subtraction, be achievable for less than $40M\$$. This figure is a "top-down" upper bound achieved by removing all items from the CKM cost estimate not required for **K***plus* . An initial "bottoms-up" estimate of

the cost of the **K***plus* detector, based on scaling the full CKM costs for revised beam-line elements, detector components and channel counts, is $\sim 25M\$$.

All total costs discussed here are in standard US HEP accounting units. These include all labor costs, contingency (typically 50%), G&A (overhead), etc. For scale, these costs are typically $\times 2.5$ the cost of materials and services alone.

4 Adaptation to an Unseparated Beam

4.1 Ideas behind this adaptation

If the beam momentum constraints of the separation system are removed, then a decay-in-flight experiment like CKM can be scaled in beam momentum by lengthening the apparatus by a momentum scale factor. Apertures, coverage, decay fractions, etc. all scale correctly. What does not scale in the CKM design are the velocity spectrometers (the K^+ and π^+ RICHes) which are tuned to particular particle velocities ($\beta\gamma = P/M$). CKM is designed to accept decay π^+'s in the forward hemisphere in the K^+ rest frame. At a higher beam momentum there is a more backward region in the K^+ rest frame where the π^+ in the lab still fall in the same lab velocity region for the same pion RICH as designed for CKM. These π^+'s have somewhat larger lab angles than in CKM making vertex resolution better and getting the π^+'s further from the beam.

The increased beam momentum allows for significant improvements in the performance of the photon veto systems. The minimum lab angle of both the accepted π^+'s and the corresponding photons from $K\pi 2$ decays on the other side of the beam from the π^+ has increased. This minimizes the photon inefficiency due to an overlap of the charged pion and a photon at the photon veto. The minimum energy π^0 will increase as minimum K^+ beam momentum exceeds the maximum π^+ momentum usable in the RICH. The photons from these high energy π^0's will preferentially hit the CsI rather than the VVS photon vetoes. The CsI has even lower inefficiencies for high energy photons ($> 1GeV$) than the conservative limit of 1×10^{-5} for lead-scintillator VVS modules which we have adopted based on our test-beam results on a prototype at JLAB where we observed 3×10^{-6} for electrons incident on the face of a module [20]. Both the increased photon energy scale and the decreased inefficiency for the highest energy photon provide important opportunities to increase the photon energy threshold.

The most obvious potential limitation of an unseparated beam is the presence in the Upstream Magnetic Spectrometer (UMS) of more than $20\times$ the K^+ flux of other charged particles in the beam. In such an experiment with a $10MHz$ K^+ flux, the UMS will have to track $\sim 230MHz$ of charged particles. The kaon fraction of the unseparated beam is now a limiting factor.

The underlying ideas for this adaptation are to double the kaon beam momentum and increase the momentum bite while maintaining a small parallel beam. The pion RICH has usable momentum resolution ($\Delta p/p < 2\%$) for pion momenta up to $30GeV/c$. With a secondary beam of $37-53GeV/c$ produced in a solid angle of $1 \times 1mrad^2 = 1\mu sr$ we have a minimum π^0 energy of $7GeV$ and a beam size in the decay volume of $(1 \times 1cm^2)$. The signal π^+'s are in the angular range $4-14mrad$ allowing a vacuum beam pipe for the un-decayed beam through the detector without acceptance loss.

The "pencil" kaon beam is an important asset. The position resolution given by size of the beam in the decay volume is comparable to the position resolution of the UMS system extrapolated to the decay point. Requiring that decay daughter tracks come from the beam is an additional constraint against miss-measurements and scatters in upstream material.

4.2 Beam

With the choice of an unseparated $37 - 53 GeV/c$ positive beam with a $1 \mu sr$ solid angle produced by 120 GeV/c protons on a 1 interaction length ($40cm$) Be target, the fluxes of particles entering a decay volume $86m$ downstream of the production target are shown in table 1 [21].

120 GeV/c *protons/sec*		4×10^{12}
secondary momentum		$37 - 53 GeV/c$
secondary transmission		50%
decay volume fluxes	protons	125 MHz
	π^+	95 MHz
	K^+	10 MHz
	total	230 MHz

Table 1: Decay volume secondary particle fluxes

The choice of positive secondary beam is based on the production cross-sections for 120 GeV/c protons on a Be target. In this secondary momentum range the kaon fraction is about 4% for either charge beam while the production cross-section for K^+ is about $5\times$ larger than for K^-. Therefore it takes considerably less 120 GeV proton flux to product the necessary kaons. In a negative beam the non-kaon component is all π^- which would have 2/3 as many interactions in the material of the upstream detectors. Negative beam remains an option at the cost of 1×10^{13} protons/sec on target, or more likely, a somewhat larger solid angle secondary beam. With the choice of positive beam the requirements for Main Injector protons to drive **K***plus* are similar to those for CKM.

The secondary beam is achromatic (no net bend) in the decay volume. This is a requirement of both the geometry of the NM2-4 enclosures and the need for a small parallel beam. The goal for the beam size is $1 \times 1cm^2$ in the decay volume with small $\sim 0.1mrad$ angular divergence. The upstream kaon decays in this beam amount to 23% which are accounted for in Table 1. Pion decays are at $1.4\times$ the rate of kaon decays.

This beam design is motivated by the existing NA48/2 charged beam whose characteristics are similar. There is an on-going effort to develop a detailed beam-line design for the NM2 enclosure. This design appears to meet all the requirements [22]. Critical details of collimation and beam tails are currently under study.

4.3 Detector

This section describes the proposed changes to the CKM detector to accomplish **K***plus* . In general terms the changes are small changes to the RICHes, DMS and veto systems. The UMS and the whole issue of kaon tracking and momentum spectrometer redundancy for the kaon measurements are significantly different.

4.3.1 Layout

The **K***plus* layout is shown in Figure 1. The coordinate system has its origin at the kaon production target (the KTeV coordinate system) and the detector elements are arranged to fit into the KTeV beam enclosure (NM2) and the KTeV detector hall (NM3-4). The region between these two enclosures is a $30cm$ ($12in$) beam pipe through a large, buried, pile of steel muon absorber. This

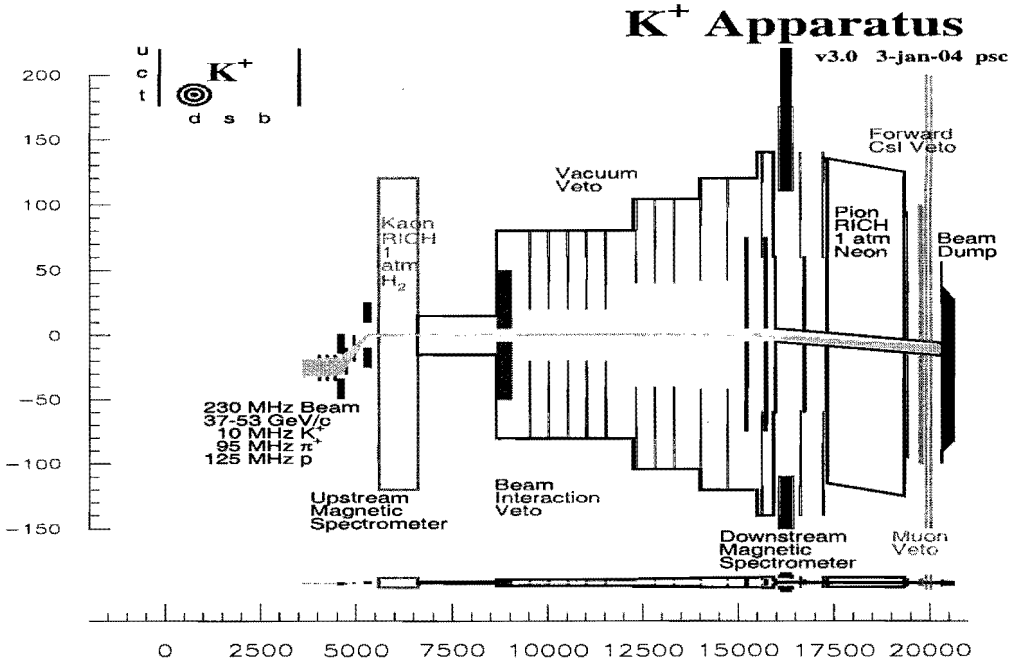

Figure 1: overall plan view layout for the **K***plus* design.

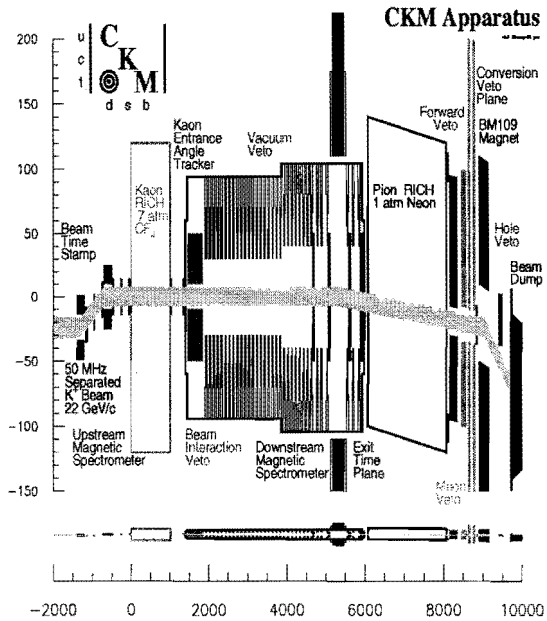

Figure 2: overall plan view layout for the CKM design.

region is shown in Figure 1 as the section of vacuum decay volume from $66 - 84m$. For comparison the CKM layout is shown in Figure 2 at the same scales as in Figure 1 directly above.

The only significant difference in the back end of these layouts is the vacuum beam pipe to allow the unseparated beam to exit without additional interactions in the **K***plus* design. The decay volume is scaled in length and the density of photon vetoes is reduced by another factor of two due to the much reduced requirements for detection of low energy photons discussed in more detail below. The kaon RICH is largely the same: the radiator gas is changed to Hydrogen at $0.9atm$ and lengthened by 20%. The large changes to the detector are the upstream magnetic spectrometer chambers and the unseparated beam itself.

4.3.2 Kaon RICH

The kaon RICH now needs to measure the velocity of beam kaons from $37 - 53GeV/c$. The working gas of choice is Hydrogen at $0.9atm$ With a $12m$ long gas volume and a single $17m$ focal length mirror with a $2cm$ diameter hole for the beam we can achieve all the requirements while minimizing the amount of material traversed by the beam. The windows on the kaon rich can be small in diameter and very thin. A critical issue is controlling the potential backgrounds from the interactions and multiple Coulomb scattering in this material. With the present design the total material traversed by the beam from the last station of UMS chambers through the kaon RICH and into the decay volume vacuum amounts to 3.8×10^{-3} radiation lengths and 3.7×10^{-3} interaction lengths. This redesign of the kaon RICH has been reported at the recent RICH2004 workshop [23].

The lowest momentum kaons have a $5mrad$ Cherenkov angle; some of the light from the last $2m$ of gas goes in the mirror hole. Due to the large momentum bite of the beam the distribution of Cherenkov photons across the phototubes is much more uniform than in CKM. We require about 300 PMTs for the kaons rings with an average rate of 300 kHz per tube.

Looking at the $95MHz$ of beam pions is very difficult. All the pion light would hit one ring of $\sim$ 100 PMTs with $\sim$ 15 photons per pion for an average tube rate of $\sim 15MHz$. Protons are below Cherenkov threshold and therefore unobservable in this counter. The kaon RICH provides a precision spectrometer for only the kaons allowing us to measure well the velocity and time of only the 4% kaon component of the beam.

4.3.3 DMS - Downstream Magnetic Spectrometer

The straw-tube planes designed for CKM will meet the **K***plus* requirements with little change. We will need to physically leave out straws that are within $5cm$ of the beam to leave room for the exiting beam pipe. There are no accepted pions to be tracked in this region so there is no acceptance loss. We will have to revisit the redundancy issue in the first DMS station where only 5 planes may not be sufficient with $10cm$ swathes missing in all views.

This system was successfully prototyped several years ago. This work is documented on the relevant CKM webpage [24].

4.3.4 Pion RICH

The pion RICH design is largely the same as for CKM. It has useful resolution ($dP/P < 2\%$) in the momentum range $14 - 30GeV/c$. There will now be the exiting vacuum beam pipe running down the middle of the radiator volume. We need to split the mirror, sending half the light up and the other half down to minimize the Cherenkov photon losses from the beam pipe obstruction. The loss from photons before they are reflected by the mirror is small; most π^+'s are at larger angles

than their Cherenkov angles in Neon. The redesign of the pion RICH has been reported at the recent RICH2004 workshop [23].

4.3.5 Photon Veto Systems

There are two main photon vetoes in these designs; a Vacuum Veto System (VVS) inside the vacuum of the decay volume and a Forward Veto System (FVS) which in either design would be the CsI array originally from KTeV. CKM also had a Hole Veto system (HVS) to detect photon which went through the beam hole in the FVS.

The minimum π^0 energy in the **K***plus* design is $37 - 30 = 7GeV$. The roles of the VVS and FVS are now inverted relative to the CKM design: in 85% of the cases at least one photon from $K\pi 2$ hits the FVS (CsI). Only $\sim 40\%$ of the $K\pi 2$ photons hit the VVS.

We will rotate the CsI by $30mrad$ to eliminate any projective cracks (the largest photon angle at the CsI is $20mrad$) we can achieve a high energy ($> 1GeV$) photon inefficiency of 3×10^{-6}:a value consistent with the latest measurements made in Japan [25]. Since we require a π^0 inefficiency of $< 1.5 \times 10^{-7}$ this implies that we can tolerate an average inefficiency on the lower energy photon from $K\pi 2$ of 5%

The **K***plus* VVS uses the 5 existing ring counters from KTeV, which have square holes, together with 3 large and 5 small VVS modules of the CKM design where the small modules now have $20cm$ radius holes rather than the $30cm$ radius planned for CKM. The reduced efficiency required for low energy photons will allow us to use 2mm thick lead plates, similar to the 2.5mm thick plates which were used in the existing modules from KTeV. This reduces the amount of scintillator and wavelength shifting fiber per module by a factor of two relative the CKM design. The original CKM design for the VVS was prototyped and tested over several years [26, 27] culminating test in an electron beam at JLAB [20] where it significantly over-achieved the original, conservative, CKM inefficiency goals for $1GeV$ photons.

We've simulated the π^0 inefficiency as we did for CKM. We set a photon energy threshold of $> 60MeV$, including a $700MeV$ (2 MIP) threshold in the CsI and remove the BM109 magnets and HVS accepting 100% inefficiency for photons in the beam hole. We can achieve a π^0 inefficiency of 1.0×10^{-7}, somewhat better than the values of 1.5×10^{-7} achieved in the CKM design. With a minimum threshold of $60MeV$ the electronics and rate challenges in the photon veto systems are much reduced. Questions regarding veto rates from thermal neutrons, which were raised in the CKM design, are now moot.

4.3.6 MVS - Muon Veto Systems

The CKM muon veto systems (MVS) is now augmented by the existing KTeV muon vetoes. With this addition the MVS is over-specified; its requirements will be reviewed. A piece of the of the R&D program will be to measure the rejection of the existing KTeV system, which will inform how the existing system needs to be augmented. We expect the scope and cost of this augmentation will be significantly less than the MVS design in the CKM proposal. Achievable MVS performance was established in a test beam effort for CKM at IHEP several years ago [28].

4.3.7 UMS - Upstream Magnetic Spectrometer

The original MWPCs planned for CKM have little hope of handling $230MHz$ of unseparated beam. There is a region in the achromat where the charged particles are dispersed over an area $7 \times 2cm^2$ or $\sim 17MHz/cm^2$. The Saclay group has developed a new kind of detector to play the role of UMS chambers in NA48/2 experiment. "KABES" is a TPC-type detector using micromegas as

an amplification gap. It has operated reliably in up to $20MHz$ of charged beam flux with beam spot sizes of $\sim 4.5cm^2$ [29]. These chambers drift ionization perpendicular to the beam axis so the appropriate scaling is by the width of the beam perpendicular to the drift direction; $7cm$ in our case. Direct scaling of the NA48/2 results would allow us to operate at $60MHz$. We need to push this technology another factor of < 4 in rate to allow operation at $230MHz$. In high rate studies at NA48 we have operated KABES at up to $6-7\times$ the nominal NA48/2 beam rate with no operational chamber problems [30]. These chambers put very little material in the beam; typically of order 10^{-3} radiation lengths per $\{x, y, t\}$ measurement station. Spatial and time resolutions of $100\mu m$ and $0.8nsec$ respectively have been achieved in NA48/2.

In order to provide redundancy for a KABES-like UMS system, we plan to use BIVS as an active collimator to veto beam track that scatter in the kaon RICH gas or other upstream material. BIVS is $30m$ downstream of the kaon RICH. Assuming we make the BIVS hole $10cm$ in diameter, $10\times$ the size of the beam, any charged track that scatters or produces charged or neutral secondaries at angles $> 1.7mrad$, will be vetoed by BIVS. The total interaction rate in the kaon RICH is $\sim 1MHz$. While this would be a significant veto rate, it is $10\times$ less than the $10MHz$ veto rate we planned from upstream muons in the CKM design.

With the small $1\times 1cm^2$ beam in the decay volume the spatial resolution of an upstream tracking system extrapolated $\sim 100m$ from the measurement into the middle of the decay volume will be comparable to the position resolution given by the size of the beam there. The kaon RICH also does not (and did not) have sufficient angular resolution to usefully resolve the beam divergence. These two systems form a redundant pair of magnitude of momentum and magnitude of velocity measurements of the kaon. With KABES for the UMS chambers each should give a independent time measurement with resolution for a track or ring much better than $1nsec$.

A critical issue to resolve in **K***plus* is to understand and demonstrate control of the potential backgrounds from the high flux of pions and protons in the unseparated beam. In the CKM design the only important interaction backgrounds were from K^+ interactions in upstream material and residual gas. These were estimated at < 4.0 and < 2.1 background events respectively. In the CKM background evaluations we included $7.5MHz$ of pions and protons and found no significant accidental backgrounds. Re-evaluating the probabilities for an accidental overlap of a good non-decaying kaon and all combinations of interaction and miss-measurement of $30\times$ the flux of untagged pions and protons does not yield an important new source of background.

The set of measurements which underlie simulation packages, like those contained in GEANT, are not adequate to critically assess backgrounds like these. For example, the probability that a proton or pion beam gas interaction produces a π^+ with $\sim 1/2$ the beam momentum and no other observable charged or neutral particles has not been well measured. Single particle yields are well measured but detection of the rest of such an interaction is detector dependent. This uncertainty is a major motivation for the R&D program proposed below to demonstrate that such backgrounds are, in fact, under control.

The first layer of our defense is BIVS which assures that any pion scatter large enough to get into the acceptance region with lab angle $> 4mrad$ can't come from a scatter in the kaon RICH region without traversing BIVS. It takes a minimum of an accidental time coincidence with a kaon plus at least two other mishaps (scatter, interaction, mis-measurement) to generate a background. Without heroics we can probably achieve a resolution of the time difference of the pion and kaon RICH ring of $0.5nsec$. With a $\pm 2\sigma = 2nsec$ timing cut on this quantity and a beam particle every $4nsec$ half the kaons will be free of such accidental backgrounds. The out of time tails will measure all these accidental backgrounds. But, we need to know they are small enough.

4.3.8 Detector Systems Removed

The Beam Time Stamp (BTS), Kaon Entrance Angle Tracker(KEAT), Exit Time Plane (ETC) and Conversion Veto Plane (CVP) have all been removed simply because none of these scintillating fiber or wire chamber planes can handle the $\sim 230MHz/cm^2$ beam rate. Their functions are largely covered by BIVS as an active hole veto in place of the KEAT and the lower kaon flux and higher photon veto thresholds of the **K***plus* design.

The BM109 and Hole Veto System (HVS) were removed both to make the detector fit an NM3-4 and because we could afford to ignore the photons in the beam hole without compromising the overall π^0 inefficiency.

The removal of the Kaon Entrance Angle Tracker(KEAT) system is an important loss in defending against backgrounds from beam interactions in upstream material. The KABES technology detectors will handle, at the hardware level, full beam rate at the entrance the vacuum decay volume. Whether the resulting data will be at net win or loss in controlling backgrounds, due to confusions in pattern recognition, etc. is unclear. We plan to leave space for a KEAT station but will make no claims for it now. Obviously that material will be replaced by a Helium bag if it isn't a net asset in suppression of background.

5 Design and Simulation of a KABES based UMS

This section presents the proposed layout of the **K***plus* Upstream Magnetic Spectrometer (UMS), the required performance, and simulation results. The simulation includes important effects such as multiple scattering, chamber response, and effects related to multiple tracks in a 230 MHz secondary beam.

5.1 Introduction and Requirements

The Upstream Magnetic Spectrometer is designed to measure the momentum and trajectory of the K^+ as it enters the decay volume. The UMS is used together with the K^+ velocity measurement from the kaon RICH (KRICH), the measurement of the π^+ trajectory and momentum from the Downstream Magnetic Spectrometer (DMS) and pion RICH (PRICH), to achieve the best possible recoil (missing) mass measurement. The expression for the mass recoiling against the π^+ is:

$$M^2_{miss} = M^2_K(1 - \frac{p_\pi}{p_K}) + M^2_\pi(1 - \frac{p_K}{p_\pi}) - p_K p_\pi \theta^2 \tag{3}$$

where θ is the angle between the K^+ and π^+ momenta in the lab frame and p_K and p_π are the respective magnitudes. The missing mass reconstruction is used to kinematically reject the dominant 2-body decay backgrounds: $K\pi 2$ and $K\mu 2$.

Of these two, the $K\pi 2$ background is more troublesome. The M^2_{miss} of the $K\pi 2$ background overlaps substantially with M^2_{miss} of the $\pi^+\nu\bar{\nu}$ signal.[1] The photon veto system is expected to reject the π^0 in $K\pi 2$ decays at the 10^{-7} level. The relative branching ratio between the signal and $K\pi 2$ background is expected to be 3.3×10^{-10}.

We can now estimate the kinematic rejection of the $K\pi 2$ background needed for a S/N=10 in 'Region-I'. The detector geometrical acceptance to the π^+ is similar for $K\pi 2$ and $\pi^+\nu\bar{\nu}$ decays. The kinematical acceptance of $\pi^+\nu\bar{\nu}$ is about 16% in Region-I. Therefore, to achieve a S/N = 10,

[1]The M^2_{miss} of $K\mu 2$ events, using the hypothesis that the μ^+ charged daughter is a π^+, is substantially far away from the M^2_{miss} signal. In addition, the μ^+ is identified by the PRICH and DMS combination, and independently by the Muon Veto System (MVS).

the kinematical acceptance to $K\pi 2$ needs to be less than 5.28×10^{-5}. As we will see later in this document, the simulation shows that the UMS design meets this requirement.

5.2 Detector Technology

A challenge for the UMS is to track 10 MHz of kaons in an environment of 220 MHz of other charged particles. The tracking chambers must be sufficiently thin to minimize multiple scattering and interactions. The detector must be efficient to tracks in this high-rate environment, and the response must be sufficiently fast. We plan to use technology similar to the KABES [31] system developed by the Saclay group for NA48/2. These are gas-based TPC's where the gain stage is performed by a single micromegas mesh [32].

Figure 3 shows the principle of operation. A single UMS chamber consists of a 10 cm x 10 cm x10 cm volume of gas such as CF_4-ethane. Since the P940 beam consists of nearly parallel tracks, we arrange the beam to enter through the center of this cube and parallel to the z-axis. The ionized electrons are drifted by a uniform E-field (parallel to the x-axis) towards a micromegas mesh and an anode strip plane. The anode strip pitch is 800 μm. The gap between the mesh and anode strip is 25 μm.

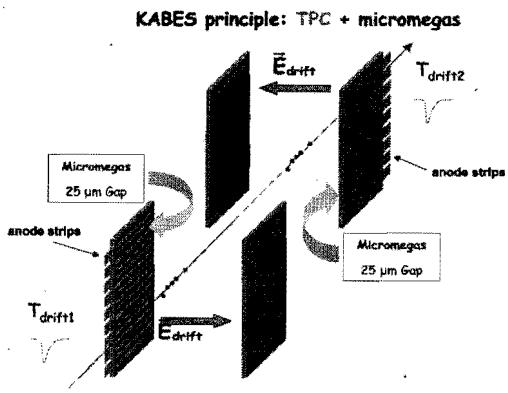

Figure 3: The operating principle of the NA48/2 KABES device.

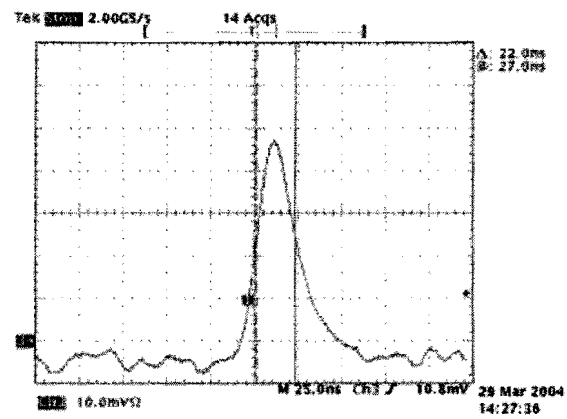

Figure 4: Pulse shape response of a 25 μm gap micromegas mesh to a Fe^{55} source [33].

This design has several significant advantages, as is summarized in the following few paragraphs. The TPC concept allows for a 1-d space and time measurement derived from a single hit, allowing for a relatively compact electronics readout system. The chambers are relatively thin, as the tracks traverse two 25 μm kapton windows and 10 cm of CF4-ethane.

Because we arrange the beam to be parallel to the anode strip direction, the ionization electrons of a given track will drift into the mesh almost *simultaneously*; the initial size of the electron cloud and gas diffusion are the dominant sources of time dispersion. This is very different than the situation in conventional wire chambers in which ionization clusters drift times are vastly different. A track traversing 10 cm of CF_4-ethane will deposit about 3000 electrons that drifts coherently onto the micromegas mesh.

The gas amplification occurs in the 25 μm gap between the micromegas mesh and the anode strip plane. This process produces intrinsically short pulses. The anode strip current consists of a fast electron current, and a slower ion-return current. However, in the micromegas amplification process, ions travel about 25 μm. Therefore, unlike wire drift chambers, where the ions typically

travel a distance of order millimeters to centimeters, ions are swept out of the gain region rather quickly. Figure 4 shows a pulse shape from the NA48/2 KABES.

5.3 Detector Layout

The UMS consists of 10 chambers (figure 5): 6 and 4 chambers on either side of a dipole analysis magnet. The analysis magnet is part of an achromat, where the bend views are in the vertical direction. The chambers are oriented such that the ionization electrons drift in the horizontal view. The odd-numbered chambers drift electrons in the +x direction, the even-numbered chambers drift in the -x direction. The time when a chamber hit is observed depends on the event time (i.e. track arrival time at the chamber), and on the drift time of the ionization electrons (i.e. the x-coordinate). In a single chamber, it is not possible to resolve this ambiguity. However, in an arrangement of chambers with alternating drift directions, this ambiguity can be resolved. A fit can be made to hits for 6 track parameters: 5 spatial parameters consisting of x_0, θ_x, y_0, θ_y, p, and the track time t_0.

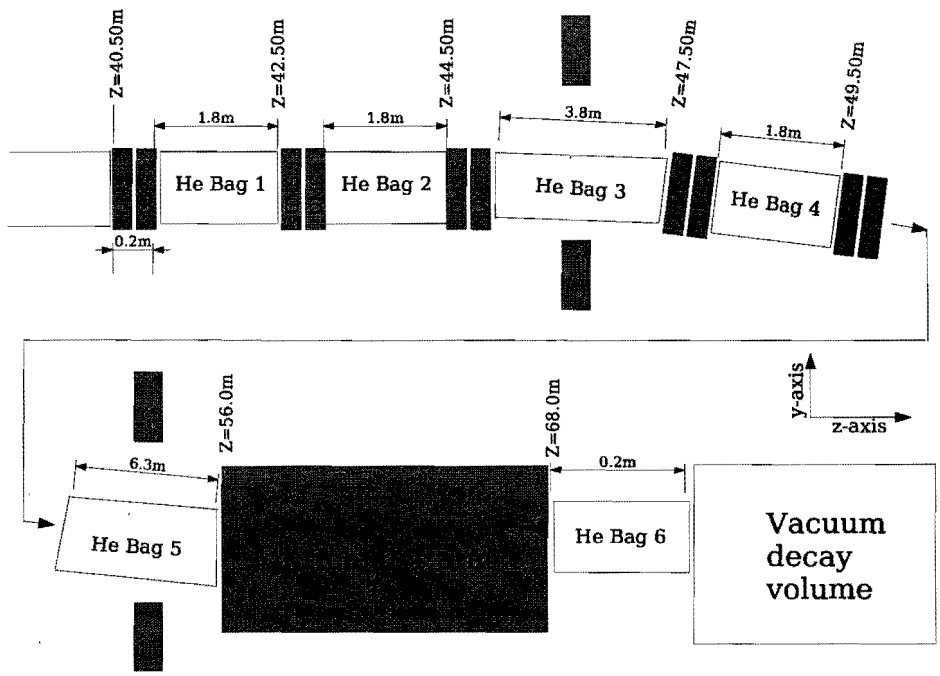

Figure 5: Layout of the detectors upstream of the vacuum decay volume. The dipole magnets shown are the last two magnets of an achromat. The figure is not drawn to scale.

The beam and achromat are important for the UMS performance and reconstruction. To first order approximation, the beam enters the achromat with a momentum bite of 37-53 GeV with zero divergence. The pencil beam is dispersed by the upstream achromat as it goes through the UMS chambers, and then is recombined back into a pencil beam by the downstream achromat before it enters the KRICH. This reduces the single rate on the UMS anode strips. Since the beam has almost zero divergence, there is a strong correlation between the track momentum and the strips that are hit. As will be shown later, this is useful in the pattern recognition.

It is important to minimize the material upstream of the vacuum decay volume. Each pair of UMS chambers consists of 5 25 μm kapton windows and 20 cm of CF_4-ethane. Each helium bag and the KRICH have 2 25 μm kapton windows. The vacuum decay volume has a 575 μm (23-mil) kevlar window. The material content from the first UMS chamber to the vacuum decay volume is 16.5×10^{-3} X_0 and 11.6×10^{-3} λ_0. Figure 6 shows the relative material contributions.

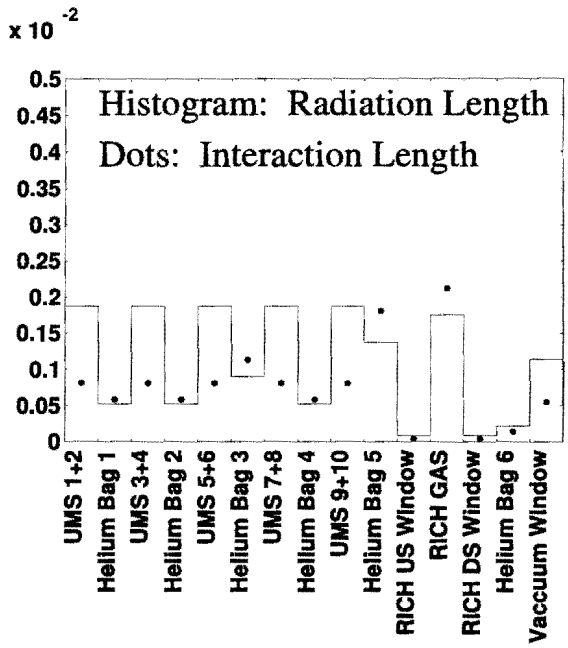

Figure 6: The contribution of material in the detectors upstream of the vacuum decay volume. The histogram (dots) indicate the amount of radiation (interaction) length. The total radiation and interaction length is 16.5×10^{-3} X_0 and 11.6×10^{-3} λ_0 respectively.

5.4 Simulations and Results

We use two simulation packages, described in the following two sections, to predict the performance of the UMS. In particular, we check the response of the UMS to $K\pi2$ events and see how the detector imperfections contribute to $K\pi2$ background. In these packages, the other tracking detectors (KRICH, DMS, PRICH) are simulated as having Gaussian resolution functions. And multiple scattering was not simulated for the daughter π^+. This is done in order to study the UMS contributions to resolution and tails in isolation.

5.4.1 Multiple Scattering in the Upstream Detectors

A simulation package, based on GEANT-3 and FLUKA, is used to predict multiple scattering of the K^+ tracks in the material from UMS-1 to the kevlar window upstream of the vacuum decay volume. The K^+ decay to $\pi^+\pi^0$ is subsequently generated in the vacuum decay volume. The scattering includes both multiple Coulomb and hadronic scattering, and the production of secondaries. In the case where secondaries have been generated, the secondaries are traced through the detector without any energy deposits. This is conservative, as we expect to have some sensitivity to vetoing the secondaries.

The amount of material simulated is shown in figure 6. Single K^+ tracks are traced through this material. There is no attempt to simulate the UMS time response and pattern recognition. The response of the UMS detectors (i.e. the UMS hits) are simply the actual x and y positions of the tracks smeared in a Gaussian fashion by 140 μm in y (bendview), and 100 μm in x (non-bendview). The UMS track hits are processed by a 5 parameter fit to extract x_0, y_0, θ_x, θ_y, P_K, and a fit χ^2.

Figure 7 shows the K^+ angular and momentum resolutions, which are nearly constant over the range of 37-53 GeV/c. The tracks were selected to have a reduced $\chi^2 < 4$. The figure also shows the simulation without scattering. As we will see later, events in the non-Gaussian tail are due mainly to scattering in the material contained in UMS-9 to the vacuum window. The scatters that occur in the region between UMS-1 to UMS-8 are rejected by the requirement on track fit quality. The events that remain are scatters that cannot be discriminated by this χ^2 requirement.

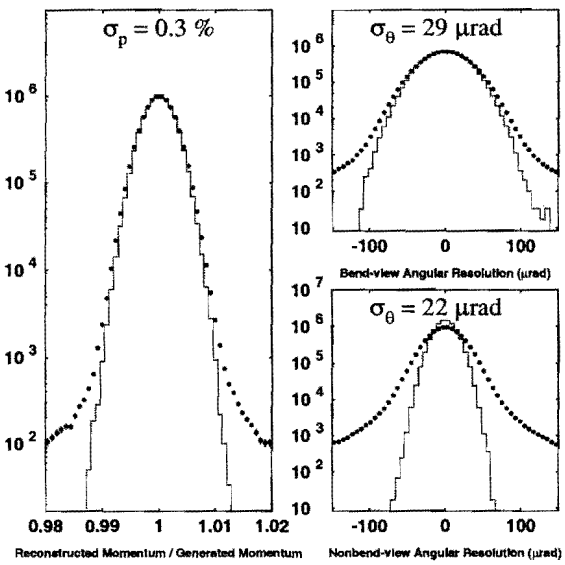

Figure 7: The momentum and angular resolution of the reconstructed K^+ in the UMS. The tracks were selected to have reduced $\chi^2 < 4$. The dots (histogram) show the effect with (without) multiple scattering simulation.

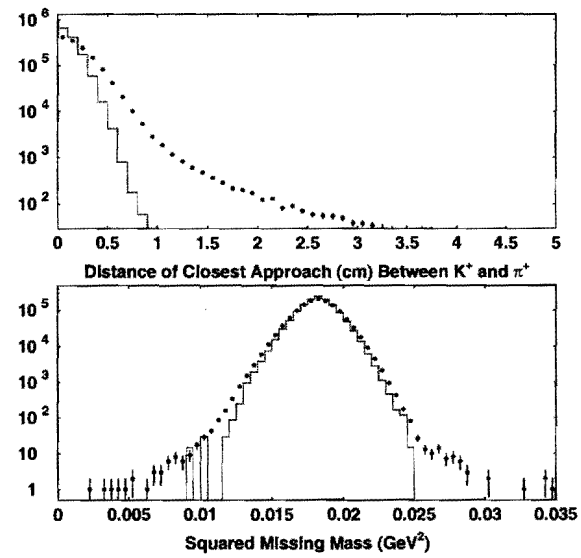

Figure 8: The Distance of Closest Approach (DOCA) and the M^2_{miss} for $K\pi 2$ events. The dots (histogram) show the quantities with (without) multiple scattering simulation. For the simulation of the π^+ response, only Gaussian detector responses were simulated (i.e. no multiple scattering in DMS or PRICH).

On the other hand, scatters occurring in the region from UMS-9 to the vacuum window can be suppressed by requiring that the K^+ and π^+ tracks form a good decay vertex. The good-vertex variable is the distance-of-closest-approach (DOCA) between the reconstructed K^+ and π^+ tracks. For scatters, DOCA can be inconsistent with that of a good vertex since the K^+ track direction was mis-reconstructed. If the decay plane, defined as the plane that contains both K^+ and π^+ tracks, coincides with the scattering plane, then DOCA cannot be used to reject these scatters. Figure 8 shows the DOCA resolution, with and without scattering simulation. This mechanism was studied and documented in the CKM proposal.

It is important to identify the main differences between **K***plus* and CKM upstream detectors. Each **K***plus* UMS chamber is about 1/2 the material of a CKM UMS chamber. However, there is no plan currently to have a Kaon Entrance Angle Tracker (KEAT), which would have been installed

immediately upstream of the vacuum decay volume window. Because of the lack of the KEAT and the desire to minimize interactions, the **K***plus* upstream design makes every effort to minimize the KRICH material seen by the beam. The beam waist in the KRICH is small (1 cm x 1 cm) and goes through a hole in the mirror. The KRICH gas is H_2 at atmospheric pressure, and so the windows can be made of 25 μm thick kapton.

We can now examine the $K\pi 2$ background due to K^+ scattering in the upstream material. Figure 8 shows the M^2_{miss} when the K^+ is subjected to scattering in the upstream material. The events satisfy $p_\pi > 13$ GeV/c, $\theta_\pi > 6$ mrad, and DOCA < 1 cm. For the simulation of the π^+ response, only Gaussian detector responses were simulated (i.e. no multiple scattering in DMS or PRICH). [2]

As shown in figure 8, the number of events in region I, defined as $-0.004 < M^2_{miss} < 0.008$ GeV^2, is 14 events out of 1.3M events. This represents a region I kinematic rejection factor of $(1.1 \pm 0.3) \times 10^{-5}$ events. We can now examine which of the upstream material is contributing to the background. For these events, figure 9 shows the p_t imparted by the upstream material. The p_t of the scatters are in the range 20-40 MeV/c. There is also no single dominant scattering source.

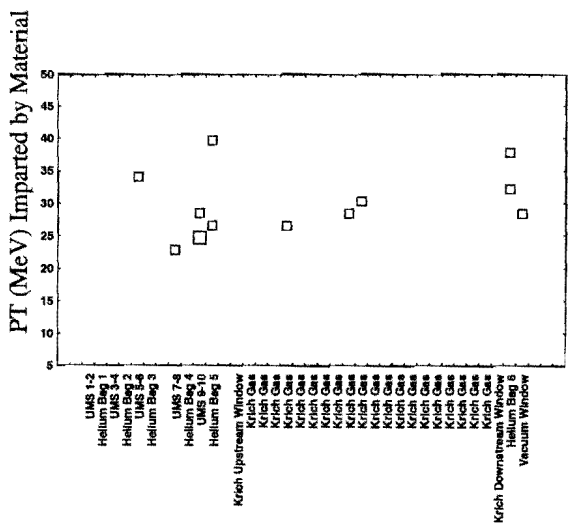

Figure 9: For the $K\pi 2$ events that scatter in the upstream material, and become background in the Region-I signal region, the figure shows the p_t (MeV) imparted by the material.

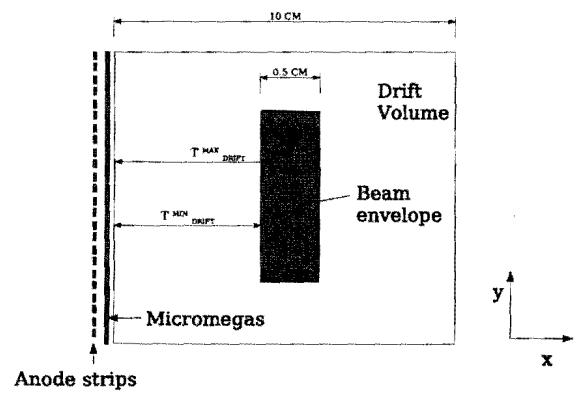

Figure 10: Minimum and maximum drift times in a UMS chamber. Given a drift velocity of 100 μm/nsec, T^{MIN}_{drift} and T^{MAX}_{drift} are 475 nsec and 525 nsec respectively.

5.4.2 Accidental Effects

The UMS must be able to track the K^+ in a 230 MHz beam. A simulation and pattern recognition package is used to evaluate K^+ tracking in this high rate environment. The goal is to determine the tracking efficiencies and mistakes in the K^+ reconstruction. These mistakes are propagated into a $K\pi 2$ simulation, where we evaluate how often these mistakes cause the $K\pi 2$ to become background to $\pi^+\nu\bar{\nu}$. The multiple scattering was not simulated, so that the effect of accidentals could be

[2] All effects are included in the background estimates in Section 8 below.

studied in isolation. These two background mechanisms are independent so their background contributions will just add linearly.

The overall strategy goes as follows. A K^+ track will trigger the KRICH, and deposit hits in the UMS. The pattern recognition must sift through all the extra UMS hits that are present due to the other tracks. The first step in the simulation is to determine how many extra tracks to generate, and their arrival times at the UMS chambers. The simulation assumes a uniform beam free of micro time-structure. In the next step, we simulate the UMS hits (space and time) due to each track. We make the UMS hit simulation as realistic as possible. Detector response functions were modeled from data taken in August 2004 with $25\mu m$ KABES detectors in the NA48 beam. Next, the UMS hits from all tracks are merged into a single event record. The event record is processed by a pattern recognition and fitting program, in which we evaluate the efficiencies and tracking corruptions. In the final step, these tracking results are propagated into a $K\pi 2$ simulation, where we evaluate how often the corruptions can cause $K\pi 2$ to become $\pi^+\nu\bar{\nu}$ background.

5.4.3 Generation of Track Multiplicity and Times

The KRICH trigger determines when the K^+ track arrived at the target (t_0). An event is defined as a set of UMS hits consistent with being in-time with the KRICH trigger. A UMS hit (t_{hit}) is defined as being in-time if it satisfies:

$$t_0 + t_{flight} + T_{drift}^{MIN} < t_{hit} < t_0 + t_{flight} + T_{drift}^{MAX} \tag{4}$$

The value t_{flight} is simply the flight time from the target to the UMS station in question. The values T_{drift}^{MIN} and T_{drift}^{MAX} are the minimum and maximum possible drift times of the ionized electrons. These values depend on the location of the drift-view of the beam centroid and width, and on the drift velocity of the gas. This is diagrammed in figure 10.

The simulation uses an electron velocity in CF_4-ethane is 100μm/nsec, a chamber drift dimension of 10 cm, a beam that is centered in the drift view, and a beam width of approximately 0.5 cm in all UMS chambers.[3] Therefore, we have:

$$T_{drift}^{MIN} = \frac{47500\ \mu m}{100\ \mu m/nsec} = 475\ nsec \qquad T_{drift}^{MAX} = \frac{52500\ \mu m}{100\ \mu m/nsec} = 525\ nsec$$

The time window of $T_{drift}^{MAX} - T_{drift}^{MIN} = 50$ nsec allows for accidental tracks to deposit hits that can be considered to be in-time. For example, a track arriving 50 nsec earlier than t_0 can deposit an in-time hit if the hit drift time is T_{drift}^{MAX}. This happens if the track hits the outer edge of the beam envelope. Similarly, a track arriving 50 nsec later than t_0 can deposit an in-time hit if the hit drift time is T_{drift}^{MIN} (inner edge of beam envelope). Therefore, to simulate the proper amount of extra hit activity, we simulate random tracks that strike the target within ± 50 nsec of t_0.

In a time window of ± 50 nsec centered about the K^+ track, there are an average of 23 tracks distributed randomly without micro-structure. The K^+ arrival time at the target can be set to $t_0 = 0$ nsec, without loss of generality. After this change, the target arrival time of the other tracks can be determined. The target arrival time of all tracks found, after setting the K^+ arrival time to $t_0 = 0$ nsec, is shown in figure 11.

[3]The simulation uses a beam divergence of 100 μrad x 100 μrad. Given that the Z-location of the last UMS station is about 50 meters, the beam width is 0.5 cm

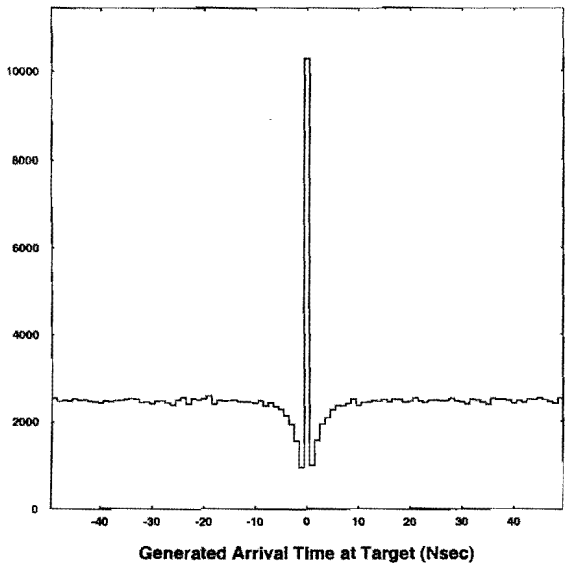

Figure 11: The time of arrival of all tracks at the target. The K^+ track arrival time is set to $t_0 = 0$ nsec (spike at 0 nsec), without loss of generality.

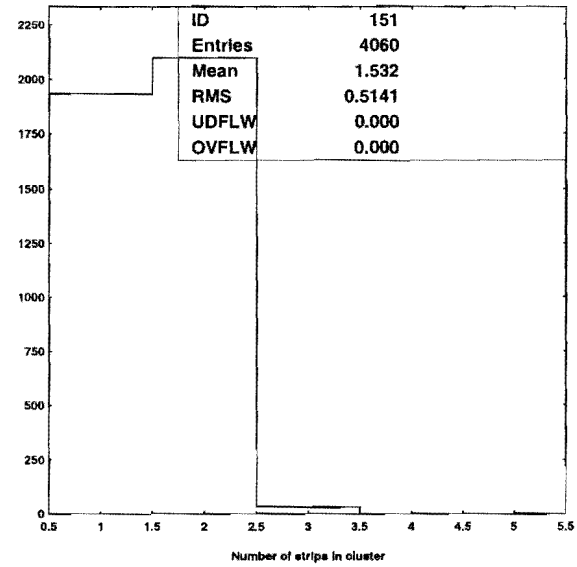

Figure 12: The number of strip hits per track in a single UMS chamber (strip multiplicity).

5.4.4 UMS Hit Simulation and Hit Merging

This section describes the simulation of UMS hits for single tracks, and the overlay procedure. The UMS response to single tracks are parameterized from the August 2004 testbeam data of the NA48/2 KABES system [34]. The KABES anode strip currents were amplified, discriminated, and sent to a TDC system in which both the leading and trailing times were digitized. A few of the amplified signals were also sent to 500 MHz FADC's. The apparatus included a mixture of 50 μm and 25 μm gap micromegas. We use data from only the latter.

A sample of charged tracks were cleanly identified in low-intensity data. From this sample, we measured the strip multiplicity and pulse width distributions, and the time resolutions. The strip multiplicity refers to the number of strip hits per track in a single UMS chamber. It reflects the cluster-size of the ionization, and is controlled by effects such as gaseous diffusion and strip pitch. Figure 12 shows the multiplicity to be either 1 or 2 strips. The pulse widths are simply extracted from the difference between the leading and trailing edge TDC measurements (figure 13).

The time resolutions were measured using events in which a single track deposits charge on an adjacent pair of strips (doublets). In particular, the time difference between the hits on these strips (figure 14) has a mean of zero, but the variation is depends on the intrinsic hit's time resolution. For the 25 μm gap micromegas, the intrinsic time resolution per hit is about 1 nsec, and the dependence on pulsewidth is negligible. As shown in the figure, we also model the non-Gaussian tails of the time resolution. The hit efficiency was essentially 100% and so did not require a detailed modeling.

To summarize, for each track we generate a track time according to figure 11, and then generate the track hits according to figures 12, 13, and 14. An event is defined as the record of all hits from all tracks. If there are two hits on a strip that are sufficiently close in time, then a simple procedure is used to decide whether to merge the two hits into one. Let t_L^1 (t_L^2) and t_T^1 (t_T^2) be the leading and trailing edges of hit 1 (2). If $t_T^2 < t_L^1$, then the two hits are merged into a single hit of leading

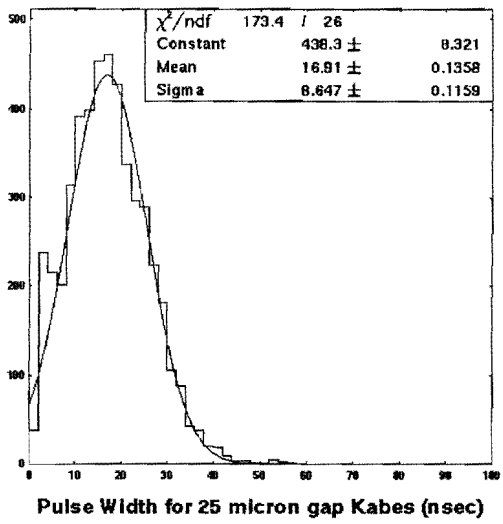

Figure 13: The pulsewidth distribution (nsec), defined as the time difference between the leading and trailing TDC edges. The Gaussian fit shows our simulation, and we constrain the simulated pulsewidth to exceed 5 nsec.

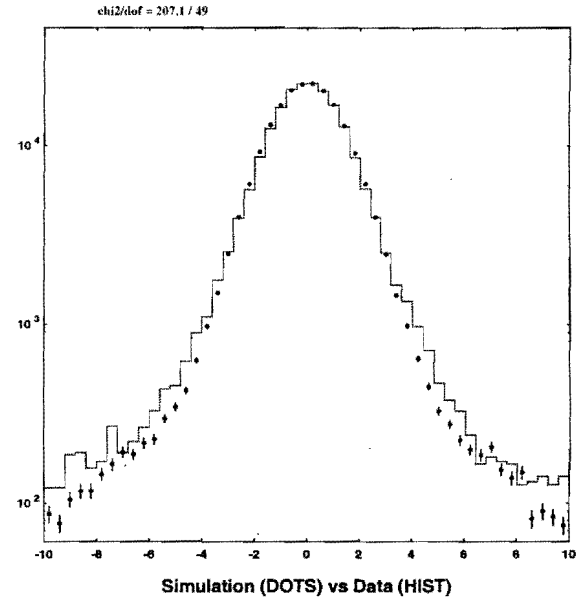

Figure 14: The time difference (nsec) between hits in a doublet (see text). The intrinsic time resolution per hit is approximately 1 nsec, with negligible pulsewidth dependence. The histogram (dots) shows the data (simulation).

edge t_L^1 and trailing edge t_T^2.

5.4.5 UMS Pattern Recognition and Fitting

This section describe the tracking algorithm. Readers can simply skip to the next section to see the tracking results. The most important thing to keep in mind is that the tracking reconstruction relies heavily on our knowledge of the beam phase space.

Since the event hit multiplicity is rather large, the pattern recognition has to be kept simple and robust. A track in the UMS is described by 6 parameters: 5 track spatial parameters consisting of x_0, θ_x, y_0, θ_y, p, and the track time t_0. Given an arbitrary set of these 6 parameters, one can make a prediction of the strip and leading edge[4] time coordinates of each hit in each UMS chamber. If there exist a hit that agrees with the space and time predictions within resolutions, then it is entered into an array of 'candidate hits'. The track fitting procedure is simply to use the candidate hits and invert a 6x6 matrix and to obtain a fit χ^2. In principle, one can scan over all possible parameters in this 6d space, and find all tracks. This would be a simple and robust procedure. It is brute-force, since there is actually no pattern recognition being done.

The pattern recognition that we shall use is similar to this brute-force procedure, but we take advantage of our a-priori knowledge of the beam phase space and the KRICH time in order to reduce the space of the parameter scanning. The KRICH gives the t_0. Since the tracks come from a point source, x_0 and y_0 can be taken to be the coordinate of the secondary target. The parameter θ_y affects the strip coordinate. But since the beam divergence is rather small (100 μrad), and the

[4]In principle, we can predict trailing edges as well.

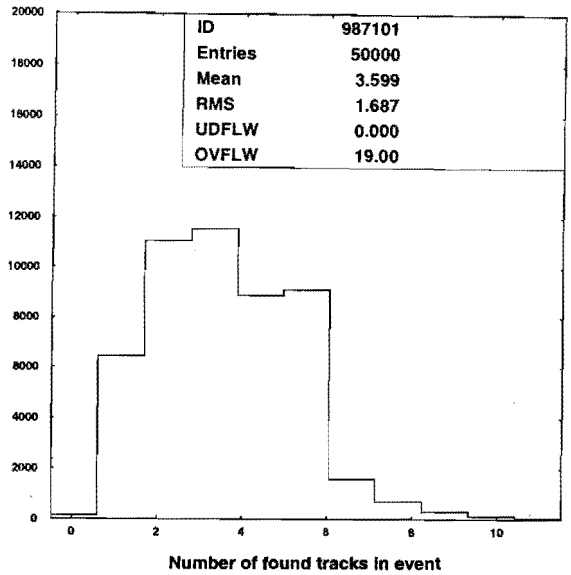

Figure 15: Distribution of the number of tracks found per event.

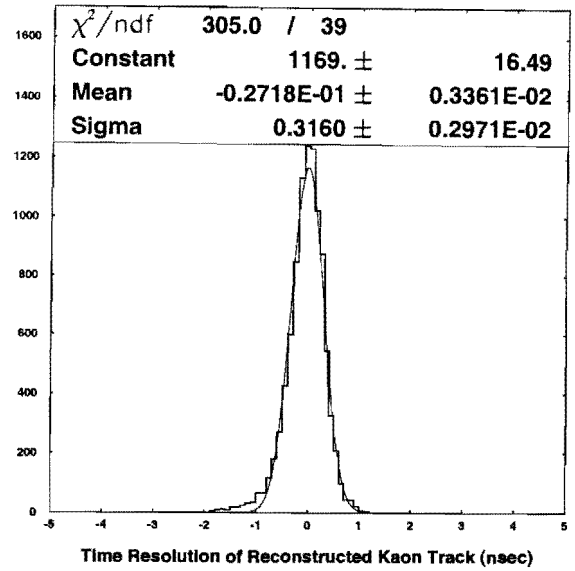

Figure 16: The reconstructed time (nsec) of the K^+ tracks, where the simulated time was 0 nsec.

strip pitch is 1 mm, we effectively scan over θ_y by allowing candidate hits to be $\pm$ 3 strips within the prediction of $\theta_y = 0$. So the 6d search space has been contracted to a 2d search space, leaving only θ_x and p.

The 2d scan over θ_x and p is simplified further by using hits in UMS1 as 'seed' hits. In other words, we do not need to search over all possible θ_x and p, but only those parameters that would predict the strip and time coordinates of the UMS1 hit. Given the drift time of a hit in UMS1, we can predict a θ_x since we have t_0 (from the KRICH) and x_0 (point source beam). Given the strip coordinate of a hit in UMS1, we predict p by using the knowledge of y_0 (point source beam), the assumption of $\theta_y = 0$, and the achromatic beam optics.

To summarize, a track is described by 6 parameters, which predicts the strip and time coordinates of hits in all UMS chambers. The task of the pattern recognition is to make an array of hits (candidate hits) that agree with the predictions within resolution. By using the knowledge of the beam phase space and modest assumptions, the number of unknown parameters is reduced to 2 (θ_x and p). Next, we recognize the fact that a hit in UMS1 can be used to predict θ_x and p. So a hit in UMS1 is used to predict the 5 parameter values (t_0 is already given by the KRICH), which in turn predict the strip and time coordinates in the remaining UMS chambers. The array of candidate hits is formed by hits whose strip and time coordinates agree with the prediction within resolution.

The candidate hits are sent to a track fitter, which inverts a 6 x 6 matrix to re-extract the 6 parameters. Since the bend view is orthogonal to the drift view, the problem reduces to inverting two 3 x 3 matrices. The inversion of one 3 x 3 matrix extracts t_0, x_0, θ_x, and χ_1^2. The inversion of the other 3 x 3 matrix extracts y_0, θ_y, p, and χ_2^2. The total χ^2 is simply $\chi_1^2 + \chi_2^2$.

The final crucial step is to refine the list candidate hits using Chavenet's criteria. With very high hit multiplicities, the candidate hit list will contain hits from different tracks. A hit is removed from the candidate hit list if its χ^2 contribution exceeds 5. The candidate hit list is re-fitted to get updated track parameters and the fit χ^2. One searches again for hits that have $\chi^2 > 5$, and remove them from the candidate hit list. The candidate hit list is re-fitted yet again. The procedure

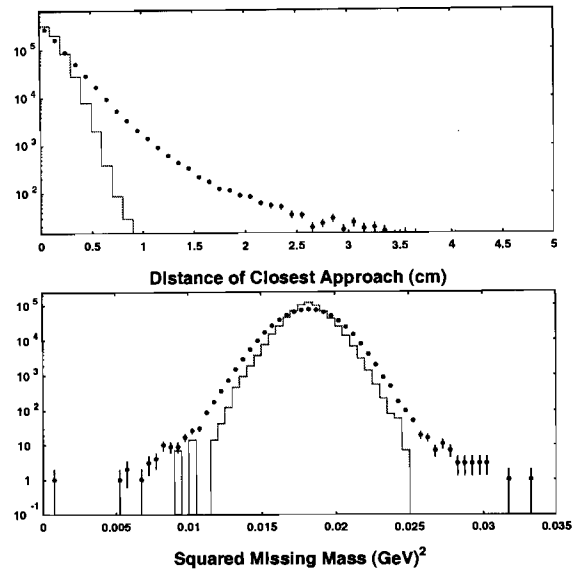

Figure 21: The Distance of Closest Approach and M^2_{miss} for $K\pi 2$ events. The dots (histogram) show the reconstruction with (without) the 250 MHz charged particle environment.

5.5 Chamber Aging in KABES

Our knowledge of the KABES radiation damage is bounded from NA48/2 data. Our rough estimate is that the upstream NA48/2 KABES stations have been exposed to 6.4×10^{12} charged particles. At this dosage, there were no observed degradations. At the August 2004 NA48/2 testbeam, which took place at the end of the NA48/2 program, we measured a $> 95\%$ hit efficiency for the upstream KABES stations. Over 3 years of running, the K*plus* UMS stations will have been exposed to 2.6×10^{15} charged particles. So the NA48/2 KABES charged particle dosage is 0.25% of the expected K*plus* dosage.

The KABES geometry is such that the hadron beam does not go through the micromegas and anode strips, which see only the ionization electrons. Because of this, we should be able to study radiation damage to good accuracy with radioactive sources. The gas gain in the micromegas amplification stage is relatively low, due to the large primary ionization from each track in 10 *cm* of gas. Aging is not expected to be significant in chambers of this type for the fluences we require. Micromegas aging studies in other chambers confirm this hypothesis [35] where no aging was observed in a total accumulated charge/mm^2 comparable to what we expect. In the event that radiation damage becomes severe, we believe that we can replace the micromegas and anode strips in a straight forward fashion.

5.6 KABES UMS Summary

This section presented the proposed layout of the **K***plus* Upstream Magnetic Spectrometer. The technology is based on a 25 μm gap micromegas TPC, such as the NA48/2 KABES system. The effect of multiple scattering, including material in all upstream detectors, has been simulated. The resulting $K\pi 2$ background, due to multiple scattering effects corrupting the UMS K^+ measurement is evaluated. The region-I kinematic cuts reject $(1.1 \pm 0.3) \times 10^{-5}$ $K\pi 2$ events.

The effect of UMS tracking in a 250 MHz rate environment has been evaluated. Simulated events consist of overlays of approximately 25 single tracks, where the beam is simulated without micro time-structure. The UMS response to single tracks is taken from the August 2004 NA48/2 testbeam data.

The pattern recognition reconstructs generated tracks with 90% efficiency. It relies heavily on the knowledge of the beam phase space. It finds an average of 2.5 extra tracks per event, in addition to the K^+ track. The extra tracks are primarily ghost tracks. They are removed by checking against the KRICH time and momentum measurement, and the DOCA quality. The resulting $K\pi 2$ background in region-I, where the K^+ measurement has been corrupted by the 250 MHz environment, is $(1.3 \pm 0.4) \times 10^{-5}$.

6 Simulations

We have performed Monte Carlo simulations to evaluate the $K^+ \to \pi^+\nu\bar{\nu}$ acceptance, to study backgrounds and to estimate rates [36]. We have benefited tremendously from the experience of our CKM simulations and have concentrated our efforts on issues related to the differences in the **K***plus* and CKM experimental techniques.

We have used GEANT 3.21 as a ray trace Monte Carlo, with all processes disabled except those relevant for each study. We have implemented only a part of the **K***plus* apparatus, which is shown in Figure 22. No magnets and detectors of the upstream magnetic spectrometer (UMS) are simulated. Beam particles are generated at the Z position of the last UMS station. After that point we have modeled a good approximation (within 10–20%) of material traversed by charged particles in the acceptance of the apparatus.

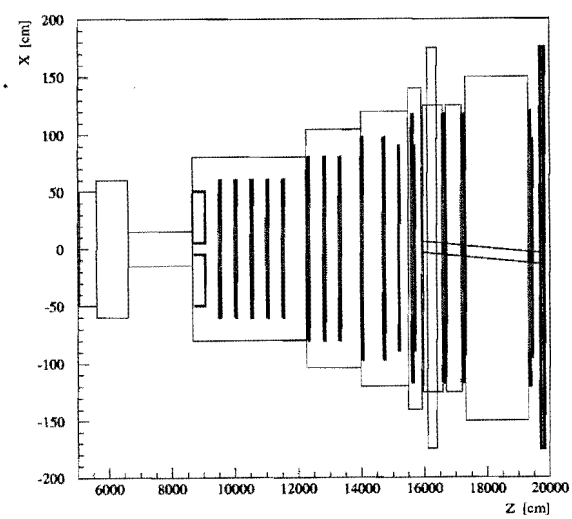

Figure 22: Downstream part of the **K***plus* apparatus.

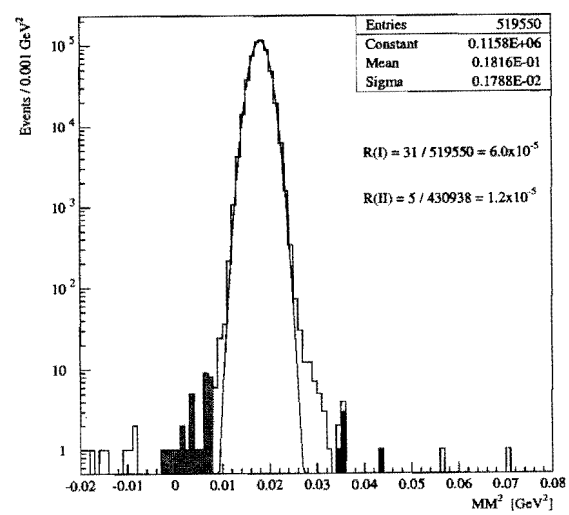

Figure 23: Missing mass squared distribution in the $K^+ \to \pi^+\pi^0$ decay for events which pass all region I selection criteria, except the missing mass squared cut. Backgrounds in regions I and II are shown hatched. Note that region II has shorter decay base.

Event selection procedures basically follows that of the previous studies for CKM. There are aperture cuts, event kinematics cuts, and reconstruction quality cuts. The cuts were selected to provide reasonable kinematic resolutions and high overall efficiency. There is clearly room for improvement, both in the description of the geometry of the experimental setup and in details of the event selection.

The backgrounds we have estimated with this technique are summarized in Table 3 (page 33). Here we briefly consider the three most important backgrounds.

6.1 The $K^+ \to \pi^+\pi^0$ background

The $K^+ \to \pi^+\pi^0$ decay is the second largest K^+ decay with a branching ratio of 21.2%. Two ways to suppress this background are by photon veto rejection and exploitation of the two-body kinematics.

In CKM this decay has been identified as the major source of background in region I. Consequently, we have paid significant attention to the $K^+ \to \pi^+\pi^0$ decay for **K***plus* .

An important feature of the **K***plus* experiment, as compared to CKM, is that there is a different π^0 energy spectrum. In CKM, only events with a minimal π^0 energy of 1 GeV can pass the selection criteria on primary and secondary track momenta, while the typical π^0 energy for passed events is 4.5 GeV. In contrast, **K***plus* uses a different charged track momentum selection, so that the minimal π^0 energy is 7 GeV, while the typical one is 23 GeV. Thus it is easier to reject photons in **K***plus* . We have determined that the integrated π^0 veto inefficiency for $K^+ \to \pi^+\pi^0$ decays in **K***plus* is 1.0×10^{-7}, for a 60 MeV minimum threshold on the photon energy.

To estimate kinematic rejection we have allowed multiple scattering and elastic hadron scattering to occur in the Monte Carlo. However, hadron scattering has been limited only to the vacuum windows and DMS straw tubes. Hadron cross sections and interactions have been modeled by GEANT FLUKA.

The fraction of $K^+ \to \pi^+\pi^0$ events which pass all selection cuts, except the cut on the missing mass squared, is 26.3% for region I and, because of a shorter decay base, a lower number of 21.8% for region II. The probability that the reconstructed missing mass squared falls into the selected region is 6.0×10^{-5} for region I and 1.2×10^{-5} for region II. The missing mass squared distributions, as well as backgrounds in both regions, are shown in Figure 23. For missing mass squared resolution we find $\sigma = 1.8 \times 10^{-3}\,\mathrm{GeV}^2$ in a Gaussian approximation.

These calculations give an effective branching ratio, for this background mode, of:

$$\mathrm{EBR(I)} = \frac{0.2116 \times 0.263 \times 6.0 \times 10^{-5} \times 1.0 \times 10^{-7}}{0.035} = 9.5 \times 10^{-12} \tag{5}$$

$$\mathrm{EBR(II)} = \frac{0.2116 \times 0.218 \times 1.2 \times 10^{-5} \times 1.0 \times 10^{-7}}{0.050} = 1.1 \times 10^{-12} \tag{6}$$

6.2 The $K^+ \to \pi^+\pi^0\gamma$ background

In the limit of very low photon energies the $K^+ \to \pi^+\pi^0\gamma$ decay is indistinguishable from the $K^+ \to \pi^+\pi^0$ decay. In particular, missing mass, which in this decay is the $\pi^0\gamma$ effective mass, is still very close to the π^0 mass. As the photon energy increases, missing mass increases as well, and the two-body kinematic rejection becomes less efficient for region II. Helping the rejection efficiency, the decay branching ratio decreases as a function of energy. Also, as the photon energy in the kaon rest frame increases, the energy in the lab frame will increase as well, thus making photon rejection more efficient.

To simulate the decay it is necessary first to select a phase space region. We have chosen the part of phase space with a $\pi^0\gamma$ effective mass corresponding to the $\pi^+\nu\bar{\nu}$ region II. Thus there is no kinematic rejection for that phase space region, and all the rejection comes from the photon veto only.

A theoretical summary of the $K^+ \to \pi^+\pi^0\gamma$ decay and specific expressions for its matrix element can be found, for example, in [37, 38]. Two basic mechanisms contributing to the decay are inner bremsstrahlung (IB) and direct emission (DE). The theoretical description of the DE component contains two (electric and magnetic) amplitudes, which have to be determined experimentally. In the most precise measurement [37] the DE contribution has been determined with about 20% accuracy. Also it has been found that interference of the two amplitudes is consistent with zero, and contributes to the branching ratio at no more than a few percent of IB.

The branching ratio as a function of the missing mass squared has been calculated by MC integration and is shown in Figure 24. For decays which fall in the region II, which is shown hatched, the branching ratio totals to 2.4×10^{-4}. The DE contribution, shown by the dashed line, is clearly small in the region II.

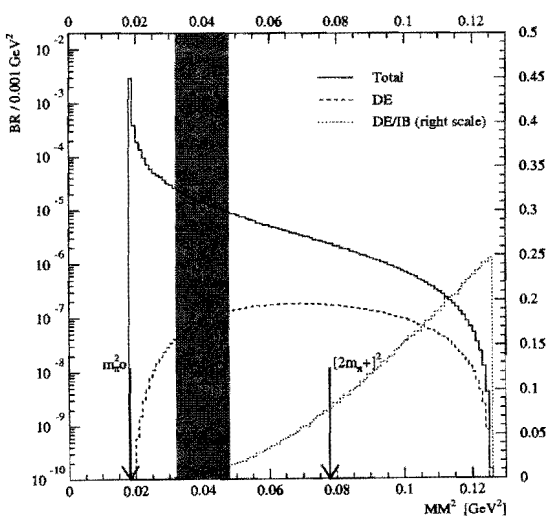

Figure 24: Branching ratio of the $K^+ \to \pi^+\pi^0\gamma$ decay as a function of missing mass squared. Nominal $K^+ \to \pi^+\nu\bar{\nu}$ region II is shown hatched.

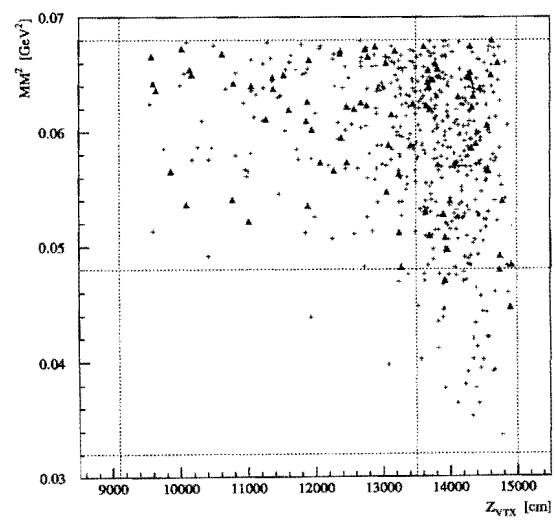

Figure 25: The $K^+ \to \pi^+\pi^-e^+\nu$ background in extended region II. Reconstructed missing mass squared versus decay Z-vertex. Dotted lines show standard and extended region II definitions. Markers show background events which pass all the standard selection criteria, with dark triangles showing events satisfying more stringent criteria: no more than 12 DMS planes with extra hits and $P_{\pi^-} < 14\,\mathrm{GeV}$.

We simulate $K^+ \to \pi^+\pi^0\gamma$ decays with all GEANT processes turned off, except for multiple scattering. The fraction events which pass standard reconstruction and selection cuts is 28.9%. The only other rejection of this decay comes from the photon veto. It has been determined with the standard photon veto inefficiency table and found to be 3.2×10^{-9}. The veto inefficiency for photons from the π^0 decay is 1.4×10^{-7}. The veto inefficiency for the internal bremsstrahlung

photon is 0.028. Combining the decay branching ratio for the chosen phase space region, kinematic reconstruction efficiencies and photon veto rejection, we arrive at an effective branching ratio for this background mode of

$$\mathrm{EBR(II)} = \frac{2.4 \times 10^{-4} \times 0.289 \times 3.2 \times 10^{-9}}{0.050} = 4.4 \times 10^{-12} \tag{7}$$

6.3 The $K^+ \to \pi^+\pi^-e^+\nu$ background

The branching ratio of the $K^+ \to \pi^+\pi^-e^+\nu$ decay is $(3.91 \pm 0.17) \times 10^{-5}$. The matrix element of this four-body decay is quite complicated [38]. We have started our analysis with a uniform phase space distribution. In region II, this background decay effectively limits the missing mass squared region we can accept for our signal.

Since $K^+ \to \pi^+\pi^-e^+\nu$ is a four-body decay, there is no kinematic rejection. However, not every point of the phase space can meet $K^+ \to \pi^+\nu\bar{\nu}$ selection criteria and produce background candidates.

For simulated $K^+ \to \pi^+\pi^-e^+\nu$ decays we have applied the standard selection procedure to the K^+ and π^+ only, ignoring the π^- and e^+. We have found that about 30% of events pass the reconstruction cuts, and out of these, 4.2% fall in the region II. Combining the $K^+ \to \pi^+\pi^-e^+\nu$ branching ratio and π^+ selection efficiencies, we can express an overall effective branching ratio as:

$$\mathrm{EBR(II)} = 9.8 \times 10^{-6} \times \mathrm{Efficiency}[e^+] \times \mathrm{Efficiency}[\pi^-] \tag{8}$$

Consequently, to keep this background to about 10% of the signal, the combined e^+ and π^- rejection inefficiency must be on the 10^{-6} level.

Rejection of the e^+ can be made by vetoing on extra hits in the photon veto detectors, pion RICH, and DMS straw tubes. The simulations have shown that in the background events which survive all the selection cuts, the electrons always either miss a VVS module or happen to be below threshold. The electron rejection inefficiency has been found to equal 2.2%. By lowering the threshold in the photon vetoes it is possible to achieve a factor of a few improvement, but not orders of magnitude. Thus, for negative pions we need to obtain a rejection inefficiency on the level of 10^{-4} or better.

We have generated a large number of $K^+ \to \pi^+\pi^-e^+\nu$ events, equivalent to 79×10^6 K^+ decays in fiducial volume. It follows that 1 event of this data set corresponds to an effective background ratio of 9.8×10^{-12}.

Most of the π^- miss the VVS. If a π^- does hit the VVS, we can safely assume that it is vetoed. We require that there is no activity in the FVS and SVS, except for the π^+ signal. We assume perfect π^- rejection if the two pions are at least 20 cm apart and no rejection if they are closer, independently of whether any of pions showers or deposits a MIP.

We use the DMS straw tubes as a veto, requiring that there are no more than 18 planes with additional hits, excluding those produced by the π^+, but including those produced by the e^+. Given the 25 ns maximal drift time, we do not expect large $K^+ \to \pi^+\nu\bar{\nu}$ inefficiencies caused by close in time charged particles.

The scatter plot of reconstructed missing mass squared versus decay vertex Z-coordinate for the selected with standard procedure $K^+ \to \pi^+\pi^-e^+\nu$ decay events is shown in Figure 25. Dotted lines show our current region II definition and an "extended" definition, in which the missing mass squared is limited by the $K^+ \to \pi^+\pi^+\pi^-$ decay and the full decay base is used.

Four events satisfy all selection cuts. In two of them the π^- is close to the π^+, in the other two the π^- goes into the FVS beam hole. This reflects a general feature of this background mode:

the π^- always goes into forward direction, and there exist only two possibilities to escape rejection: pass through the beam hole or merge with the π^+. Another feature of the remaining background, imposed by the extra DMS hits cut, is that the π^- is quite close to the beam axis. Thus if the π^- momentum is above the Cherenkov radiation threshold of 12 GeV in the RICH, some fraction of light is absorbed by the beam pipe. That makes it difficult to describe the RICH response accurately. By examining π^- momenta and path lengths in the pion RICH in these four events, we have conservatively estimated that we can reject 1.5 events out of 4. Thus, this mode corresponds to an effective branching ratio of

$$\text{EBR(II)} = 25 \times 10^{-12} \tag{9}$$

It can be lowered by cutting further on the decay volume and missing mass squared, or by employing more aggressive cuts on the number of extra DMS hits.

7 Acceptance

parameter	CKM	**K***plus*
120 GeV/c *protons/sec*	5×10^{12}	4×10^{12}
kaon momentum	$22 - 23GeV/c$	$37 - 53GeV/c$
decay volume	$19 - 42m$	$90 - 150m$
K+ decay fraction	13%	16.3%
PNN1 acceptance	$\sim 1.9\%$	3.5%
PNN2 acceptance		5.0%
total	$\sim 1.9\%$	8.5%

Table 2: Comparative acceptance estimates

We have simulated the **K***plus* geometry as was originally done for the CKM. Full details of this study are reported in Reference [36]. In Figure 26 are shown the distributions in K^+ and π^+ momentum, Z of the vertex and missing neutral mass-squared for the basic sample defining cuts: $90 < Z_{vertex}(m) < 150$ and $14 < p_{\pi^+}(GeV/c) < 30$. Since the lowest momentum beam K^+ is 37 GeV/c there is an implicit cut on the momentum of the missing neutral state of $> 7GeV/c$. The dependence of the production on K^+ momentum is included. The shaded regions of the missing neutral mass-squared plot show the definitions of PNN1 and PNN2 regions (Region-I and Region-II in the notation of the CKM proposal). The two signal regions, shown in Figure 26, are in the missing mass squared regions $-0.004 - 0.008(GeV/c)^2$ and $0.032 - 0.048(GeV/c)^2$, respectively. The PNN2 region uses only a restricted portion of the fiducial decay volume.

The acceptances in the PNN1 and PNN2 neutral missing mass-squared regions are tabulated in Table 2. The PNN1 acceptance is 3.5%, a larger that the corresponding CKM acceptance of $\sim 1.9\%$. The PNN2 acceptance is quite large (5.0%). We have not gone back and reassessed the PNN2 acceptance for CKM. It would be at least as large as the CKM PNN1 acceptance.

Figure 27 shows the pion lab kinematics for the PNN1 and PNN2 regions as well as for $K\pi 2$. All accepted pions are in the angular range from $4 - 15mrad$.

8 Signal and Background Estimates

We summarize our background studies in Table 3. Full details of this study are reported in Reference [36]. We have considered all kaon decays, and have come to conclusion that the $K^+ \to \pi^+\pi^0$

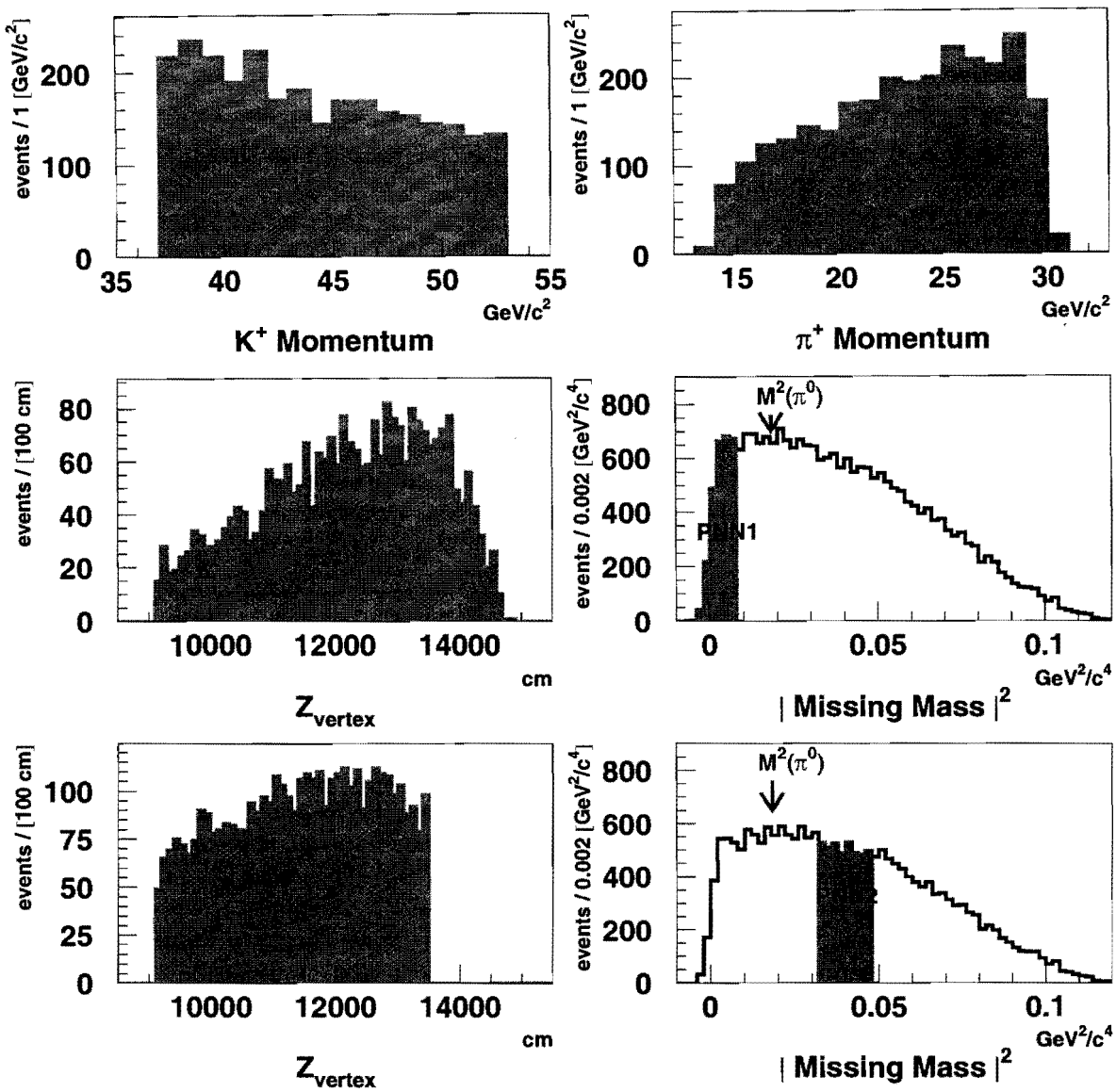

Figure 26: General acceptance properties for the $K^+ \to \pi^+\nu\overline{\nu}$ signal events. The middle and lower right plots show the distribution in missing-mass squared recoiling against the π^+. The shaded regions in these plot are the PNN1 and PNN2 signal regions, respectively. The corresponding left plots are the decay point distributions in the fiducial volume. The Z_{decay} cuts are different for the two signal regions.

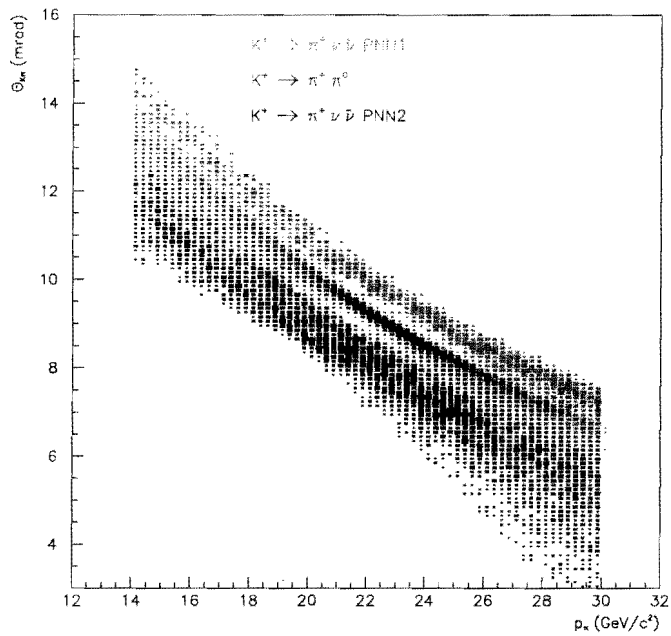

Figure 27: pion lab kinematics for K^2_π, PNN1 and PNN2.

decay is the main source of background for region I, while the $K^+ \to \pi^+\pi^-e^+\nu$ decay is the most problematic one for region II. We have considered a few accidental and interaction backgrounds and identified no significant problems so far.

Background Process	EBR (in units of 10^{-12})	
	Region I	Region II
$K^+ \to \mu^+\nu$	< 1	—
$K^+ \to \pi^+\pi^0$	9.5	1.1
$K^+ \to \pi^+\pi^0\gamma$	—	4.4
$K^+ \to \pi^+\pi^-e^+\nu$	—	25
Other K^+ decays	$\ll 1$	< 1
Accidentals in the UMS	2.0	0.3
Accidentals in the UMS and kaon RICH	1.0	0.4
Total	13	31

Table 3: Summary of backgrounds.

The study of backgrounds is not complete. We have not fully addressed all the backgrounds from pattern recognition errors and non-Gaussian resolution effects. Accidental and interaction backgrounds have been considered. However, these can not be determined with confidence with only simulations: these must be measured.

We are now quite confident in our ability to handle region II. We do not expect any new back-

grounds, associated with kaon decays. It does not mean that some intricate interaction background cannot exist which we have failed to anticipate.

In the ray tracing Monte Carlo framework used we have simulated only a few aspects of event generation and reconstruction, which are directly relevant to background studies. The true efficiency, the probability to detect a $K^+ \to \pi^+\nu\overline{\nu}$ event once it has occurred, is less than that obtained in these simulations; a value which we refer to as acceptance. Factors, causing additional inefficiency, and their expected impact, are collected in Table 4. They have been determined in stand-alone simulations, analyses of experimental data, or estimated with educated guesses. In general, selections designed to veto background contributions use different cut values in regions I and II, and corresponding efficiencies are different as well.

Origin of Inefficiency	Efficiency	
	Region I	Region II
Track reconstruction in UMS	90%	90%
Track reconstruction in kaon RICH	92%	92%
Momentum agreement for kaon track in UMS and RICH	99%	99%
Pattern recognition in DMS	98%	98%
Track reconstruction in pion RICH	98%	98%
Time agreement between UMS, DMS, pion and kaon RICHes	96%	96%
pion identification in MVS	90%	99%
pion signal in FVS is not like γ	98%	—
pion signal in FVS is not like $\pi^+\gamma$	90%	90%
pion signal in FVS is not like $\pi^+\pi^-$	—	95%
No accidentals in BVS, VVS, SVS, FVS, DMS, pion RICH	97%	94%
Total	58%	60%

Table 4: Factors and efficiencies not simulated.

We can now estimate the absolute $K^+ \to \pi^+\nu\overline{\nu}$ yield. We use following parameters and assumptions:

- 39 weeks of running per year
- 120 hours of running per week
- 3600 seconds per hour
- 6 seconds flat top every 27 seconds
- 10 MHz K^+ rate
- Decay fraction of 0.163
- Acceptances of 3.5% and 5% for regions I and II
- Additional efficiency factors of 58% and 60% for regions I and II
- Branching ratio of 1×10^{-10}

Multiplying all the values, we obtain 12 signal events per year for region I and 17 signal events per year for region II. Assuming 3 years of running we get 87 signal events and 21 background ones. All the numbers are pulled together in Table 5. Cut optimization for the region II is likely to somewhat raise the signal and/or lower the background.

YIELDS	1 Year		3 Years	
	Signal	Background	Signal	Background
Region I	11.7	1.5	35.2	4.6
Region II	17.3	5.4	52.0	16.1
Total	**29**	**6.9**	**87**	**21**

Table 5: Event yields per one and three years of data taking.

9 K*plus* Physics reach

The additional background in the PNN2 region does not significantly alter the statistical precision on the measurement of the $K^+ \to \pi^+\nu\overline{\nu}$ branching ratio. To be compelling the **K***plus* results must satisfy two criteria; demonstration of a clean signal and precision measurement of the branching ratio. We demonstrate a clean signal for the kinematically unconstrained $K^+ \to \pi^+\nu\overline{\nu}$ decay mode in the PNN1 region where the signal to noise ratio is designed to be better than 10/1. With this demonstrated we may add the events from second region, which has somewhat higher background, in order to improve that statistical precision on the branching ratio. The statistical precision of **K***plus* is 12% compared to the original CKM precision from PNN1 only of 11%.

10 Beam Requirements

This experimental program requires slow extracted, debunched, 120 GeV/c protons from the Main Injector. The proton flux necessary to produce the required secondary beam flux beam is $5 \times 10^{12}/sec$ including a factor of $\times 2.5$ over the raw cross-section for the collimation losses necessary to produce a clean beam. Debunching implies that most, but not all, of the residual 53 MHz RF structure of the beam is removed. A $\sim$ 10% residual beam modulation at 53 MHz is acceptable. A successful first attempt to operate the Main Injector in this mode was reported at the February 21, 2005 All Experimenters meeting.

The most effective way to operate the main injector to provide the beam required while still dedicating the majority of the beam accelerated to a fast spill neutrino program is a mix mode operation shown in figure 28. In this mode a long flat-top slow spill in inserted periodically in the otherwise rapid cycling fast spill program. Assuming the Main injector operates at 3×10^{13} protons per spill a 6 second flat-top allows a single cycle to be accelerated, debunched and delivered at the required $5 \times 10^{12} protons/sec$ rate. The limitation on flat-top length in the main injector is overall magnet cooling. The machine can't sustain flat-top for more than 30% of the time. The ratio of fast spills per slow spill is a program planning decision. The case shown in figure 28 balances each program at 70% of the maximum it could get running alone. This compromises each program's statistical sensitivity by $\sim$ 20% per unit running time. The effect on this proposal is to require 3 years of data taking to achieve the sensitivity above rather than the 2 years. This has been included above.

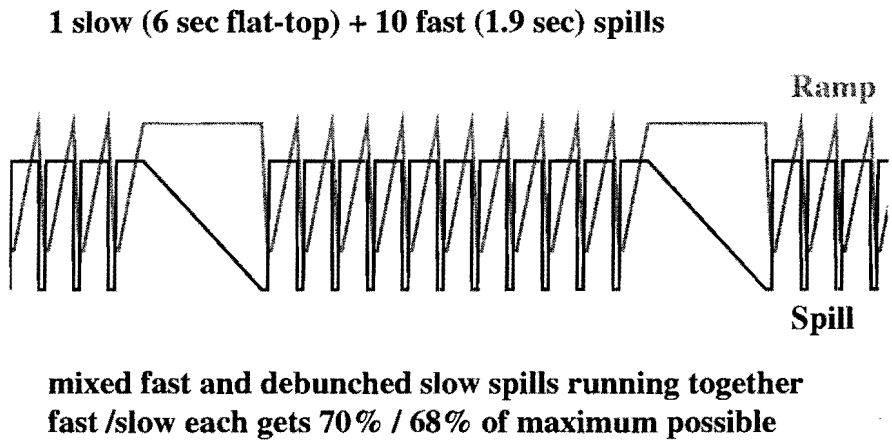

Figure 28: Mixed mode Main Injector operation mode. Blue curves are the magnet ramp and green curve the extracted beam as a function of time.

11 Critical Comparison of the CKM and K*plus* Designs

The separated and unseparated beam techniques have different strengths and weaknesses. Neither is obviously superior to the other. Some of the important differences are

- total flux $50MHz \rightarrow 230MHz$
  - Tiny non-kaon backgrounds in CKM become a small backgrounds in **K***plus* .
  - kaon - non-kaon accidentals are a concern in **K***plus* .
  - The uncertainty is simulating these backgrounds make their measurement in-situ even more important in **K***plus* .
- kaon flux $30MHz \rightarrow 10MHz$
  - The rates seen in the downstream spectrometers (DMS and pion RICH) drop by a factor of ~ 2.
  - Accidental backgrounds with a beam kaon drop by a factor of 3 in **K***plus*
  - Upstream material is substantially reduced (H_2 in kaon RICH instead of N_2 etc.). However background for these sources increases in **K***plus* because the KEAT (kaon entrance angle tracker) is had to be removed due to the high total beam flux.
- Photon veto
  - Photon energy thresholds can be increased greatly: $> 3MeV \rightarrow > 60MeV$
  - The photon spectrum from $K\pi 2$ is much harder in **K***plus* (the minimum energy π^0 goes from $1GeV \rightarrow 7GeV$). π^0's are much easier to veto.
  - With minimum thresholds of 60 MeV in **K***plus* veto activity from neutrons is a non-issue.

- The fraction of $K\pi 2$ π^0's with photons seen in the CsI goes from $10\% \rightarrow 85\%$. The CsI threshold can be set above a MIP for a large fraction of the acceptance.
- The CKM background from $K\pi 2$ photons landing on the π^+ in the CsI become negligible in **K***plus* .

- The PNN2 acceptance region (above the $K\pi 2$ peak and below the 3 body decays) has been qualified. Only a limited part of this region is usable due to backgrounds from $Ke4$. This accounts for $\sim 1/2$ of the **K***plus* acceptance. The CKM acceptance would be increased by a factor of 2 beyond the sensitivity claimed in the proposal. This was noted as possible but not claimed as part of the sensitivity in the CKM proposal.
- With the inclusion of the PNN2 region sensitivity in CKM that design has twice the sensitivity per year of data taking relative to **K***plus* .

11.1 Flexibility

A significant difference in the two designs can be found in their different potentials for adaptation in the face of challenges from backgrounds. If some background is out of control by a small factor an adaptation of the apparatus must be considered before sacrificing sensitivity to hard cuts. Our plan is to learn enough at the beam R&D stage to mitigate the disaster scenario of only finding the problem after the data is taken. Even if found at an early stage the trade-offs are still time and money. Doubling the cost and time to produce a large detector subsystem could still be fatal. The converse is that flexibility in systems where it is not required is, in the end, of little value.

11.1.1 Photon Vetoes

In CKM the photon vetoes were pushed nearly to their limits in terms of low energy photon detection inefficiency. Significant efficiency for photons as low as 3 MeV with 1 MeV of visible energy deposited in scintillator is about as low an energy threshold as is feasible with a Pb-scintillator sampling calorimeter. The CKM VVS is a major cost driver: replacing or significantly upgrading it in response to a need for great photon rejection power would be prohibitive.

In **K***plus* the VVS is identical technology but with substantially higher thresholds required. Even in the case where we would choose to reduce the amount of scintillator by a factor of 2 from the CKM design the visible energy threshold would rise from $1Mev \rightarrow 10MeV$. These thresholds are all software cuts made offline. In **K***plus* the option remains to lower those threshold globally or for some particular class of events in order to gain photon rejection power.

11.1.2 Beam Spectrometers

The CKM tracking beam spectrometer was based on conventional MWPC chambers after the HyperCP design where they operated successfully in 30 MHz of beam. 230 MHz beam flux is the major challenge to the **K***plus* design. We know from tests we have performed that KABES chambers will function at a the hardware level in much higher fluxes than this. The questions are at the level of electronics and pattern recognition. Fortunately KABES chambers are relatively small and cheap with 120 electronics channels per station and 10 stations in the design. Major modifications to this sub-system can be considered without major impacts to either time or money.

The other important issue in controlling backgrounds caused by problems upstream is material in the beam. The beam is small in area. Heroics in window materials, etc. are conceivable, subject to the safety constraints of a Hydrogen RICH counter.

11.2 Accidentals

If we have underestimated the true background rates of signal region pions from interactions of the non-kaon component of the beam then **K***plus* is at a substantial disadvantage to the CKM separated beam design. This class of backgrounds requires an accidental coincidence with a beam kaon. The kaon rate in the **K***plus* beam is 1/3 of that in CKM while the non-kaon hadronic beam rate is 30× higher. **K***plus* is an order of magnitude more sensitive to this class of background. This is mitigated by less material in the upstream beam and the option to increase the vacuum pumping capacity in order to reduce beam gas interactions if necessary.

11.3 Sensitivity

The CKM design, including PNN2 is twice as sensitive per year as **K***plus* . The limiting uncertainty in relating the $K^+ \rightarrow \pi^+\nu\bar{\nu}$ branching ratio to Standard Model parameters is the uncertainty from lack of knowledge of the charmed quark mass. For the time horizon of this measurement that uncertainty is matched by the statistical precision of a 100 event measurement. The immediate benefit is only reduced running time.

If there were compelling reasons to increase the precision of this measurement this choice would have to be revisited. When our colleagues at NA48/3 demonstrate successfully operation in a 860MHz beam then increasing the **K***plus* beam flux will be equally feasible. Increasing the per year sensitivity of **K***plus* would be at the cost of the additional protons to make that beam and modification to electronics and DAQ systems to handle the increased rates.

11.4 Summary

K*plus* is a more flexible design than CKM in several important areas. Whether this makes it a better experiment can only be known when the real backgrounds are clearly measured.

12 R&D Project

After a substantial head-start we are now in a close race to achieve these physics goals. A reasoned comparison of the relative state of advancement of the **K***plus* program at Fermilab compared to the NA48/3 program at CERN would put CERN ahead in terms of the beam; their charge kaon beamline is already operational and characterized. The **K***plus* experiment design is significantly further advanced due to having worked on it much longer. The NA48/3 effort is staffed by a highly competent and experienced group of physicists who have a demonstrated track record of undertaking and achieving difficult measurements in kaon physics. We must compete on their schedule - data taking beginning in 2009-10.

In the present environment the Fermilab director and his program committee can advance, but not approve, this or any other new experiment. Review at the national level is required with an unclear process and schedule for a decision. To embark on **K***plus* now requires a plan to maintain competitiveness with NA48/3 while the required national review unfolds. We propose to accomplish this with an R&D Project which can be undertaken in parallel with both the national review of **K***plus* and the similar NA48/3 R&D Project.

The critical issues lie ahead of each effort - demonstrating adequate background control at fixed, finite, signal acceptance. We propose to recommission the NM2-4 (KTeV) beamline as the charged kaon beam required by **K***plus* and the existing KTeV apparatus in order to characterize with measurements all the important background contributions. To this we would add two new systems

associated with the kaon beam, the KABES UMS and the kaon RICH. The KABES system is small and relatively inexpensive. We already have in hand most of the hardware we need to build the kaon RICH.

In all cases **K***plus* achieves its background rejection by two or more redundant and independent measurements. In crude terms a background rejection of order 10^{-10} is achieved by two independent measurements of 10^{-5} each. Assessing individual measurements at the 10^{-5} level requires a clean system but does not require much beam, data, or bandwidth. A list of characterizations and measurements to be made in the **K***plus* R&D Project include:

- Demonstration, development and characterization of long flat-top debunched Main-Injector beam operations
- Full characterization of the charged kaon beamline
  - kaon yield, beam content and purity
  - Detailed characterization of the beam size and tails
- Characterization of KABES operation in a full rate environment
- Characterization of the kaon RICH system in a full rate environment
- Measurement of actual scattering and interaction backgrounds
  - Multiple Coulomb scattering
  - Signal like pions from beam detector and beam gas hadronic interactions
- Quantification of photon veto performance using $K^+ \to \pi^+\pi^0$ in a limited decay volume.
- Quantification of existing muon veto performance using $K^+ \to \mu^+\nu_\mu$.

12.1 Impacts of the R&D Program

12.1.1 Primary Beamline

In switchyard 7 cryogenic dipoles need to be removed and replaced with 5 conventional dipoles. One septa station, 2 dipoles to provide the switch to the SY dump and 6 additional quadrupoles are needed. In total 14 conventional elements need to be installed. Seven of these are already stored in the switchyard tunnels.

12.1.2 Secondary Beamline

The existing target shield roof/lid must be opened (designed to do so for repair) and the existing target and beam dump plug removed. Downstream of the target in NM2 two large sweeper magnets, a 20 ft dipole and 3 collimators be removed. The installation consists of a new modest target/holder, beam dump plug, reworking of an existing collimator and 12 conventional beam elements.

12.1.3 Recommissioning KTeV Detectors

The KTeV vacuum system, drift chambers, magnet, photon vetoes, CsI and muon veto system need to be returned to operational status. All are in KTeV hall and all, save the drift chambers, are still installed in their original locations. Almost all of the electronics for these systems are still in place. There is significant technician and physicist effort required to bring these back online as an operational system.

12.1.4 New Upstream Kaon Detectors

Two new system are required both to qualify the kaon beam, themselves, and the various physics backgrounds we need to study. KABES is a Saclay invention. For now we've estimated this system as a procurement of 5 stations, 10 planes, from them. For the kaon RICH we have the vessel, phototube holder and PMTs from our RICH prototype planned for CKM. We require a mirror, a simple vacuum and gas system and 300 channels of readout.

12.2 Estimated R&D Project Costs

We are having the costs for each of these activities estimated by ADiV, CDiV and PPD staff members. Most costs are associated with labor, either Fermilab technical staff or T&M work. There is no more than 20% of the costs in materials and supplies. Work is ongoing at the time of this document on these estimates. Present values are shown in Table 6. These are fully loaded costs with a 50% contingency applied.

System	Cost
Primary Beamline	370K$
Secondary Beamline	685K$
Recommissioning KTeV Detectors	450K$
New Upstream kaon Detectors	480K$
total	1985K$
contingency (50%)	990K$
Total	2975K$

Table 6: **K***plus* R&D Project cost estimates

13 Requests

1. Scientific approval to advance **K***plus* for consideration by the national review process.
2. Prompt institution of the **K***plus* R&D project to re-establish at Fermilab the capability for a world competitive program of kaon physics.
3. Recognition that for a 3 year period beginning around 2009 **K***plus* will require 30% of the Main Injector timeline for debunched - slow extracted spill. Advancement of **K***plus* is commitment on the part of Fermilab to provide the proton beam required to yield a measurement on a competitive timescale.

14 Conclusions

Executing an *"elegant world-class quark flavor physics experiment, which would be able to produce important physics results."* ought, surely, to be well within the mission of both Fermilab and our collaboration. With the adaptation of the CKM experiment to the **K***plus* unseparated beam design we can mitigate the cost by a large factor of the measurement of the $K^+ \rightarrow \pi^+\nu\overline{\nu}$ branching ratio plus a long list of other searches and measurement in both π^+ and K^+ decay. This should address the financial concerns which have been raised.

We seek support and encouragement to advance this critical part of the Fermilab, and the world's, experimental program. Fermilab has been a world leader in kaon physics since the inception of the lab. **K***plus* is the vehicle to carry leadership in this area forward into the future.

If either Fermilab or the DOE is unwilling or unable to advance **K***plus* we then seek help and support to join our colleagues at CERN to advance this physics program as members of NA48/3.

References

[1] "CKM 10 page Facilities Description prepared for HEP Facilities Committee", February 7, 2003
http://www.fnal.gov/projects/ckm/documentation/public/10pg.pdf

[2] CKM Proposal, June 4, 2001
http://www.fnal.gov/projects/ckm/documentation/public/proposal/ckm_proposal_2nd_edition−v2.7.pdf

[3] CKM website
http://www.fnal.gov/projects/ckm/Welcome.html

[4] P940 presentation at the Femilab PAC, April 3, 2004
http://www.fnal.gov/projects/ckm/documentation/public/ckm2 − pac.pdf

[5] P940 submission to the Femilab PAC, April 2, 2004
http://www.fnal.gov/projects/ckm/documentation/public/ckm2 − pac − apr04.pdf

[6] Evgueni Goudzovski, "First results on direct CP violation asymmetry measurement in $K^{\pm} \to \pi^+\pi^-\pi^{\pm}$ decays from NA48/2", CERN Particule Physics Seminar, 1th Mar 2005.

[7] "Letter of Intent to Measure the Rare Decay $K^+ \to \pi^+\nu\overline{\nu}$ at the CERN SPS", D. Munday et al.. CERN-SPSC-2004-029, CERN-SPSC-I-229, Oct 2004. 56pp http://agenda.cern.ch/askArchive.php?base=agenda&categ=a043551&id=a043551s21t1/document

[8] Augusto Ceccuci, "Letter of Intent to Measure the Rare Decay $K^+ \to \pi^+\nu\overline{\nu}$ at the CERN SPS", Talk presented at the CERN SPSC Villars Meeting, September 27, 2004. http://agenda.cern.ch/askArchive.php?base=agenda&categ=a043551&id=a043551s21t1/transparencies

[9] G. Isidori, *private communication*, March 23, 2005.

[10] W. J. Marciano and A. Sirlin, "Radiative Corrections to π_{l2} decays", Phys. Rev. Lett. **71**, 3629 (1993).

[11] E. Frlez et al., "Precise Measurements of the Pion Axial Form Factor in the $\pi^+ \to e^+\nu_e\gamma$ Decay", hep-ex/0312029, December 9, 2003.

[12] D. Pocanic et al., "Precise Measurements of $\pi^+ \to \pi^0 e^+\nu_e$ Branching Ratio", hep-ex/0312030, December 9, 2003.

[13] V. N. Bolotov *et al.*, "The Experimental Study Of The Pi- → E- Anti-Neutrino Gamma Decay In Flight," Phys. Lett. B **243**, 308 (1990).

[14] D. I. Britton *et al.*, "Measurement of the $\pi^+ \to e^+\nu$ branching ratio," Phys. Rev. Lett. **68**, 3000 (1992).

[15] G. Czapek *et al.*, "Branching Ratio For The Rare Pion Decay Into Positron And Neutrino," Phys. Rev. Lett. **70**, 17 (1993).

[16] L. G. Landsberg, "Overview Of The CKM Physics Opportunities Beyond $K^+ \to \pi^+\nu\overline{\nu}$," Phys. Atom. Nucl. **65**, 1749 (2002) [Yad. Fiz. **65**, 1795 (2002)].

[17] L. G. Landsberg, "Medium Rare K^+ Decays with CKM",
Talk at the Chicago Flavor Seminar, Fermilab, January 17, 2003
http://theory.fnal.gov/people/nierste/cf/Chicago_Flavor.html,
BNL Particle Physics Seminar, March 13, 2003.,
http://www.phy.bnl.gov/ partsem/02 − 03.html

[18] V. V. Kiselev, A. K. Likhoded and V. F. Obraztsov, "Contributions of leptoquark interactions into the tensor and scalar form factors of $K^+ \to \pi^0 l^+ \nu_l$ decay," arXiv:hep-ph/0204066.

[19] A. I. Ageev et al., "OKA Proposal",IHEP, Protvino, 2003.

[20] E. Ramberg, P. Cooper and R. Tschirhart, "A photon veto detector for the CKM experiment," IEEE Trans. Nucl. Sci. **51**, 2201 (2004).

[21] Peter S. Cooper, "A $K^+ \to \pi^+\nu\overline{\nu}$ experiment in an unseparated beam - I - Charged Particle Yields", CKM Note 91, December 27, 2003.

[22] R. Coleman, "A Design of an unseparated beam for the CKM-2 Experiment", CKM Note 99, April 7,2004.

[23] P. S. Cooper [the CKM collaboration], "Redesign of the CKM RICH velocity spectrometers for use in a 1/4-GHz FERMILAB-CONF-05-015-CD *Prepared for 5th International Workshop on Ring Imaging Cherenkov Detectors (RICH 2004), Playa de Carmen, Mexico, 30 Nov - 5 Dec 2004*

[24] Downstream Magnetic Spectrometer (Vacuum Straw Tracker)
http://www.fnal.gov/projects/ckm/dms/

[25] K. Sakashita, "Measurement of the photon detection inefficiency due to photo-nuclear interaction",
http://pubweb.bnl.gov/people/e926/papers/techniques/sakashita.pdf

[26] G.Britvich, I.Britvich, S.Golovkin, V.Kurshetsov, L.Landsberg, V.Maisheev, V.Molchanov, V.Semenov, E.Vlasov, V.Zaruchejsky, "First results from a low momentum e+- test beam at U-70 IHEP, Protvino", CKM Note 60, February 15,2002.

[27] G.Britvich, V.Molchanov, "First results from Protvino VVS prototype measurements with 1.25 and 4.44 MeV photons", CKM Note 70, September 23, 2002.

[28] S. A. Akimenko *et al.*, Nucl. Instrum. Meth. A **494**, 509 (2002).

[29] "Status Report on Experiment NA48/2", CERN/SPSC-2003-033, October 23,2003.
http://na48.web.cern.ch/NA48/Welcome/images/talks/spsc03/NA48_2_SPSC_2003.pdf

[30] We participated in high rate tests at the conclusion of NA48 in August 2004.

[31] Bernard Peyaud, contribution to the Vienna Conference on Instrumentation, February 2004.

[32] There is a tremendous amount of literature on Micromegas. See for example the seminal paper by Y. Giomataris, NIM **A419** (1998) 239-250.

[33] Figure courtesy of E. Mazzucato of the Saclay, NA48 collaboration.

[34] CKM Note 103 - NA48/2 Testbeam Memo in draft.

[35] J. Miyamoto, S. Kane, J. May and I. Shipsey, "An aging study of a MICROMEGAS with GEM preamplification," Nucl. Instrum. Meth. A **515**, 261 (2003).

[36] Vladimir Molchanov, "The $K^+ \to \pi^+ \nu\overline{\nu}$ measurment - simulations for the P940 Geometry, CKM Note 102, March 15, 2005.

[37] S. C. Adler *et al.* [E787 Collaboration], Phys. Rev. Lett. **85**, 4856 (2000) [arXiv:hep-ex/0007021].

[38] L. Maiani, G. Pancheri and N. Paver, "The second DAPHNE physics handbook. Vol. 1, 2,"